UCID-19047

# JPLAXD: A FINITE ELEMENT PROGRAM FOR STATIC PLANE AND AXISYMMETRIC ANALYSIS OF STRUCTURES IN JOINTED ROCKS.

by

Francois E. Heuze

May, 1981

Lawrence Livermore Laboratory



Work performed under the auspices of the U.S. Department of Energy by the Lawrence Livermore Laboratory under Contract W-7405-Eng-48.

## DISCLAIMER

# INDEX

INDEX (continued)

# LIST OF FIGURES

LIST OF FIGURES (continued) Page



LIST OF TABLES

## 1. INTRODUCTION

JPLAXD is a finite element program for static plane and axisymmetric analysis of structures in jointed rock. The code was developed by F. Heuze, starting from the plane formulations of Wilson (15)* and Goodman (1). Over the years, numerous features have been added to the plane option, such as: peak and residual behavior in the solids, with strain softening and dilatancy, peak and residual behavior in the joints, with strain softening and dilatancy, automatic reset of solid and joint compliances, RESTART mode for sequential excavation or construction, plotting routines for display of deformations and stresses, and transversely isotropic materials. In addition, the code was extended to axisymmetric analysis, including all the above developments (9). The program has been used on a variety of basic and applied rock mechanics problems as illustrated in Section 7.

## 2. PROGRAM CAPABILITIES

The capabilities and limitations of the code are:

Size:

| | | |
|---|---|---|
| . maximum number of nodes | : | 500 |
| . maximum number of elements (solids & joints) | : | 400 |
| . maximum number of joint elements | : | 200 |
| . maximum number of pressure cards | : | 100 |
| . maximum bandwidth | : | 100 |
| . maximum number of materials (solids & joints) | : | 12 |

These parameters can easily be modified by changing common block statements.

Element Library:

- 4-node linear quadrilateral
- 3-node linear triangle
- 4-node linear joint

Boundary and Initial Conditions:

- boundary displacement
- gravity loading
- nodal forces
- boundary pressures
- initial stresses

---

*Indicates reference numbers.

Material Models:

- strain softening in solids
- dilatancy in solids
- strain softening in joints
- dilatancy in joints
- isotropic and transversely isotropic solids (the anisotropic model applies to pre-failure only).

Mesh Generation:

- node generation at equal intervals on straight lines
- incremental element generation

Iteration:

- secant stiffness method for iteration to known constitutive relations of solids and joints.

Restart:

- update of coordinates and material properties, for sequential
- construction or excavation.

Plotting:

- original mesh
- deformed mesh with element stresses in each iteration
- final deformed mesh without stresses.

## 3. MATERIAL MODELS

### 3.1 Solid Materials

Pre-Failure: The solids are linear elastic up to their brittle failure. Isotropic or transversely isotropic models are available. In the transversely isotropic models, the coordinate axis of the mesh must coincide with the principal directions of anisotropy.

Compressive (shear) failure: Shear failure takes place under compression. (Fig. 1). Beyond peak strength the materials can strain-soften (Fig. 2). In plane analysis, the peak and residual strength envelopes are illustrated in the $(\tau,\sigma)$ plane in Fig. 3a. They represent the Navier-Coulomb criterion, which is also written in terms of the two principal stresses as:

peak strength : $\sigma_{1p} = 2c \tan \alpha_p + \sigma_3 \tan^2 \alpha_p$ (1)

residual strength: $\sigma_{1r} = \sigma_3 \tan^2 \alpha_r$ (2)

with : $\alpha_p = 45^\circ + \phi_p/2$ ; $\alpha_r = 45^\circ + \phi_r/2$

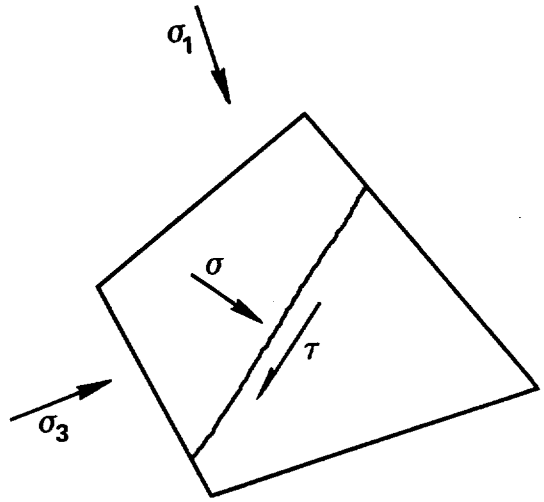


Figure 1: Shear Failure of Solids

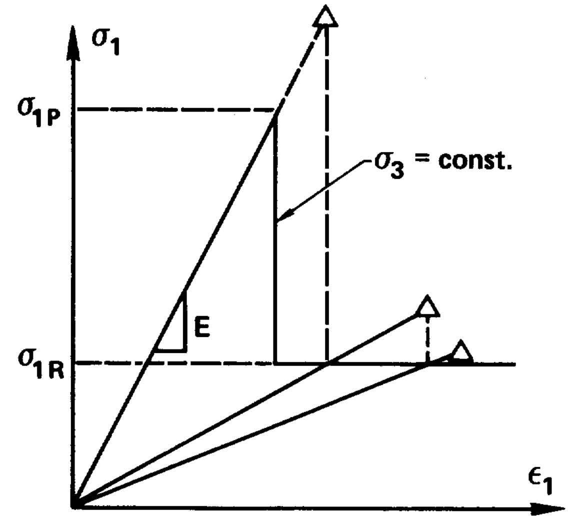


Figure 2: Strain-Softening of Solids

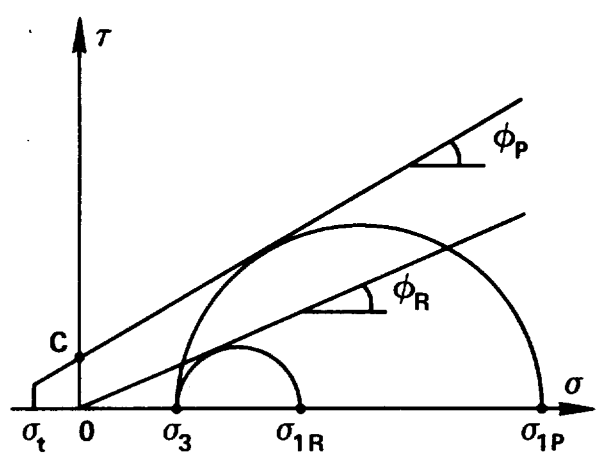


(a) Plane (Coulomb)

$$\tau_{oct}^2 = 8\,\sigma_t \cdot \sigma_{oct} \qquad (3)$$

with:

$$\tau_{oct}^2 = \left[\sum(\sigma_i - \sigma_j)^2\right]/9$$

$$\sigma_{oct} = (\sum \sigma_i)/3$$

(b) Axisymmetric (Murrell)

Figure 3: Failure Criteria for Solids

In axisymmetric analysis, there are three principal stresses. Two peak failure criteria are available in JPLAXD: the above Navier-Coulomb, and the Murrell criterion. Using Navier-Coulomb in axisymmetric cases means to disregard the intermediate principal stress. As an alternative, the Murrell criterion (Ref. 13) includes all three principal stresses. It is written in terms of octahaedral stresses in Fig. 3b. For residual strength, equation (2), above, is also used for the axisymmetric analyses. Note that Murrell's criterion for peak strength only requires the knowledge of tensile strength, $\sigma_t$. Peak friction angle, $\phi_p$, and cohesion, c, are not used; they are concepts related to the Coulomb criterion.

In the post-peak region, the solid stiffness is automatically recalculated by secant iterations, so as to conform to the stress-strain constitutive relation (Fig. 2). In the isotropic case, iterations are performed on the modulus E. In the transversely isotropic case, the material is made isotropic after failure, and iterations are performed on $E_1$.

Tensile Failure: Isotropic solids have one tensile strength, $\sigma_t$. In the Coulomb option, the tension cut-off tensile criterion is explicit: $\sigma_3 = \sigma_t$. It is implicit in the Murrell criterion. Transversely isotropic solids may have a different tensile strength in the two principal strain directions. The criterion is explicit: failure happens when $\sigma_1 = \sigma_{t1}$ or $\sigma_3 = \sigma_{t3}$. If a solid has failed in tension, its modulus is reset to a very low isotropic value. Later on, if the material is subjected again to all compressive stresses, it is reassigned an isotropic modulus calculated as

$$E = E_{original} * \frac{\text{residual strength}}{\text{peak strength}} \quad \text{at current } \sigma_3.$$

Dilatancy: the post-failure dilatancy of solids is simulated by resetting the Poisson's ratio to 0.49 in the post-peak range.

## 3.2 Discontinuities

The constitutive relations of interest for a joint in direct shear (Fig. 4), include the shear behavior (Fig. 5), the normal behavior (Fig. 6), and their coupling through dilatancy (Fig. 7).

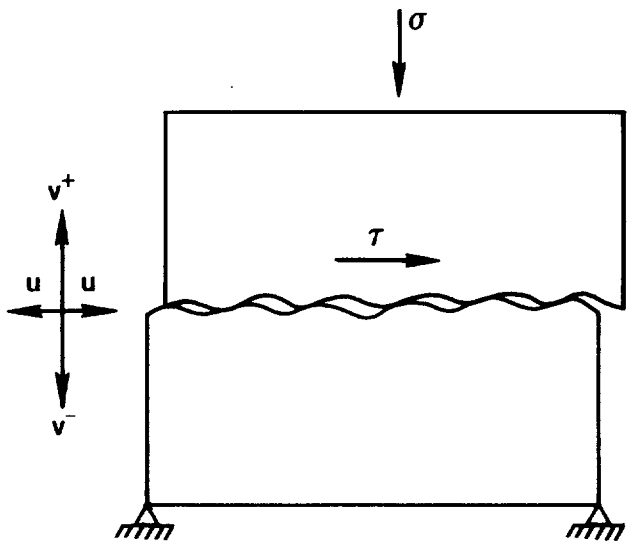


Figure 4: Nomenclature for Joints in Direct Shear.

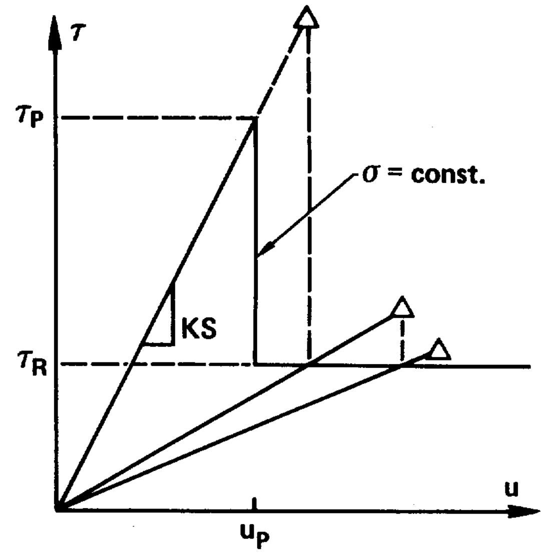


Figure 5: Strain-Softening of Joints in Direct Shear.

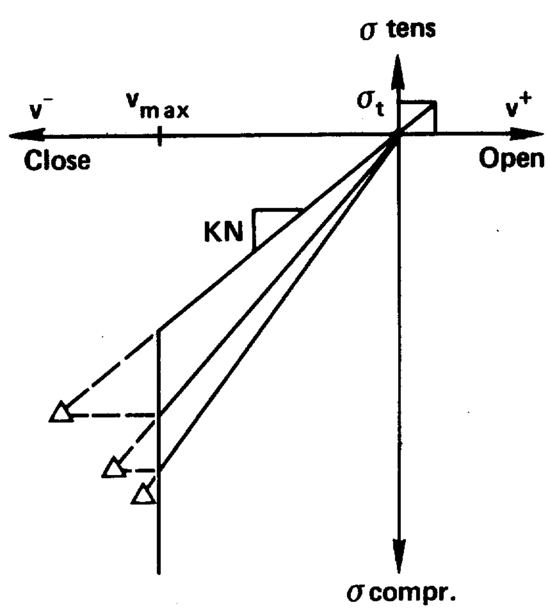


Figure 6: Joint Behavior in the Normal Direction.

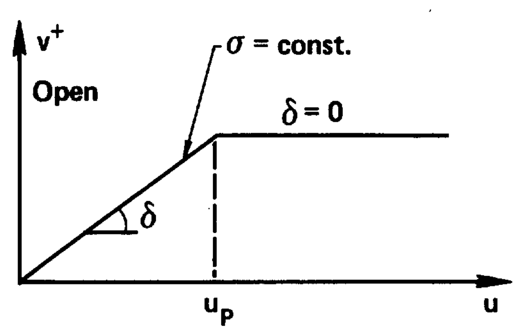


Figure 7: Joint Dilatancy in Shear.

Shear behavior: the treatment of shear behavior is similar to that described for solids in shear. There is linear behavior to peak, with a shear stiffness KS which has units of stress/length; and there is strain-softening beyond the peak. KS is automatically recalculated by secant iterations when needed (Fig. 5). The shear behavior (u direction) is considered symmetrical. The results of a series of direct shear tests at constant normal stress are summarized by peak and residual shear strength envelopes which are shown in Fig. 8.

Normal behavior: in tension, a joint may be given a limited tensile strength, $\sigma_t$, if it is healed. In most cases, the $\sigma_t$ is assumed to be zero.
In compression, joints behave linearly, with a normal stiffness KN up to a maximum closure, $v_{max}$. Again, a secant iteration is used if the calculated closure exceeds $v_{max}$. The KN is then increased progressively, as required, to meet the known constitutive relation (Fig. 6). Instead of a linear KN, one could consider a hyperbolic variation (ref. 2). However this degree of sophistication is not warranted for structural analysis, as the joint and faults exercise their influence through shear behavior and opening, and not through their closing response. When the joints are used in conjunction with fracture-flow hydraulic models, the hyperbolic representation may be desirable because the flow is very sensitive to fracture aperture.
Usually, in the three types of secant iterations described so far (1 for the solids, 2 for the joints) the convergence is quite rapid, if the structure is not globally unstable. A few iterations (4 or 5) will provide a calculated value less than 5% away from the constitutive curve.

Dilatancy: most geological discontinuities are not smooth; hence they will dilate upon shearing. The shear displacement, u, will be accompanied by a positive normal displacement, $v^+$, when asperities ride over each other. The dilation angle, $\delta$, is taken as a constant when the normal stress is constant during shear (Fig. 7). However, $\delta$ decreases as the normal stress increases. This is why the peak strength envelope of Fig. 8 has a steadily decreasing slope, up to the point where $\sigma$ reaches a critical value, $\sigma_c$, beyond which dilation is prevented; above $\sigma_c$, asperities are sheared through their base. With non-dilatant joints, there is only one envelope: the peak envelope collapses onto the residual.

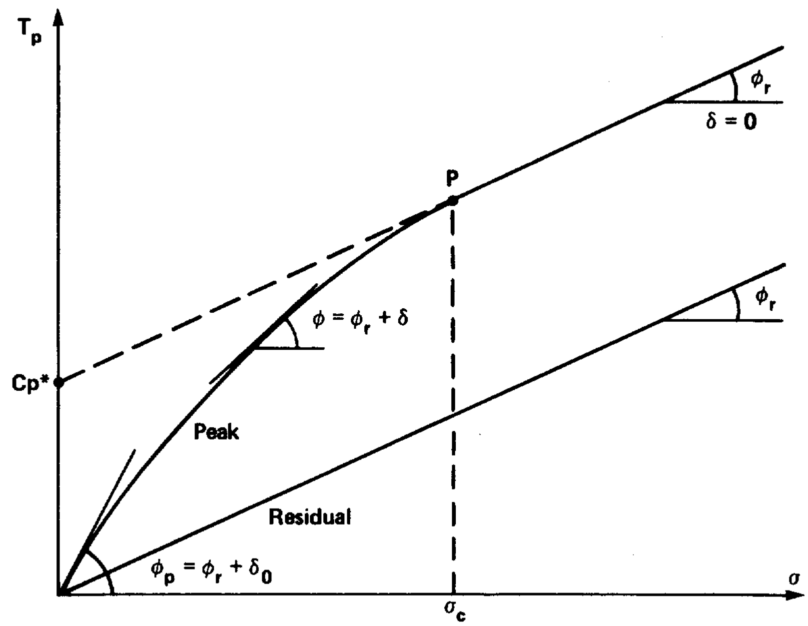


Figure 8: Peak and Residual Joint Shear Strength Envelopes.

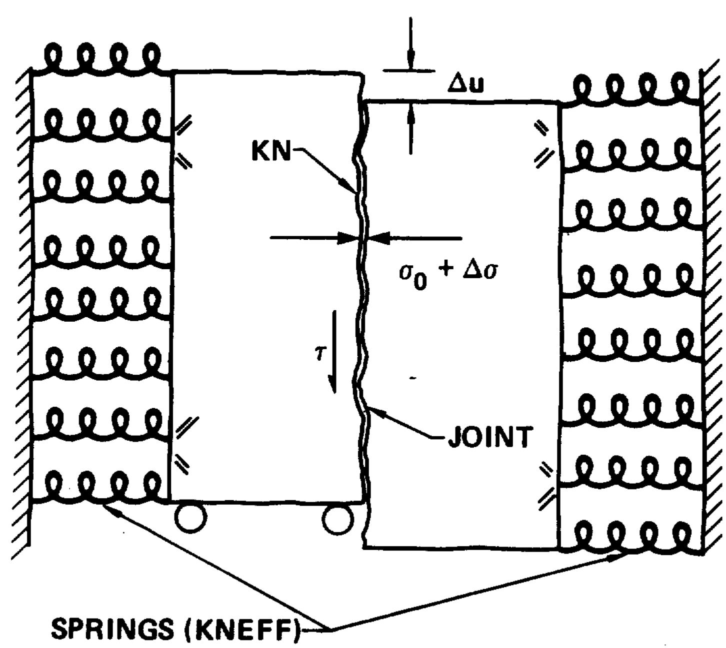


Figure 9: Conceptual Model of a Joint in Transversely Restrained Shear.

Dilatant effects: if the joint is restrained transversely during shear, by reinforcement or by adjacent rock blocks, dilatancy will induce an increase in normal stress on the joint plane. Then, the shear behavior becomes non-linear before the peak. JPLAXD incorporates a theory for dilatant behavior, which evolves from the conceptual model of Fig. 9. The theory is given in references 7 and 9. The stiffness of the transverse restraint, KNEFF, is automatically calculated in JPLAXD during the first iteration of a dilatant analysis. The calculation is based on relaxing a small excess normal stress put into each joint, from a position of equilibrium.

## 4. STRUCTURE OF JPLAXD

The JPLAXD code contains a main program (JPLAXD) and 25 subroutines. The calls to the routines and the functions of the subroutines are as follows:

### 4.1 Subroutine calls

| | | | | | | |
|---|---|---|---|---|---|---|
| JPLAXD | ←→ | INMAT | | | | |
| | ←→ | NODE | | | | |
| | ←→ | ELEMNT | | | | |
| | ←→ | PLOT1 | ←→ | NPLOT | | |
| | ←→ | RESSTR | | | | |
| | ←→ | DILAT | | | | |
| | ←→ | STIFF | ←→ | QUAD | ←→ | TRISTF |
| | | | | or AXQUAD | | or AXTRI |
| | | | ←→ | PLNJT | | |
| | | | | or AXIJT | | |
| | | | ←→ | MODIFY | | |
| | ←→ | BANSOL | | | | |
| | ←→ | DISPL | | | | |
| | ←→ | STRESP | ←→ | QUAD | ←→ | TRISTF |
| | | or STRESX | | or AXQUAD | | or AXTRI |
| | | | ←→ | PLOT 2 | ←→ | NPLOT |
| | | | ←→ | RCSGTH | | |
| | | | ←→ | PLOT3 | ←→ | NPLOT |
| | ←→ | JTSTR | ←→ | DLTSIG | | |
| | | | ←→ | JTSGTH | | |

## 4.2 Subroutine functions

JPLAXD: Main program. Calls subroutines.

INMAT: Reads control information and material properties.

NODE: Generates nodal points omitted on input. Keeps track of the nodal coordinates through all successive runs.

ELEMNT: Reads or generates element information. Calculates structural bandwidth. Inputs boundary pressures.

PLOT1: Plots the original mesh.

NPLOT: A routine to call CALCOMP subroutines.

RESSTR: Reads and/or calculates initial residual stresses; always called on a RESTART.

DILAT: Calculates the initial dilation angle and shear stiffness, for dilatant joints.

STIFF: Main routine to assemble the global structural stiffness matrix, and the global load vector.

QUAD: Formulates the stiffness matrix of a plane quadrilateral.

AXQUAD: Formulates the stiffness matrix of an axisymmetric quadrilateral.

TRISTF Formulates the stiffness matrix of a plane triangle.

AXTRI: Formulates the stiffness matrix of an axisymmetric triangle.

PLNJT: Formulates the stiffness matrix of a plane joint. Three different options are available.

AXIJT: Formulates the stiffness matrix of an axisymmetric joint.

MODIFY: Modifies the displacement vector for known displacements.

BANSOL: Equation solver. Produces the displacements.

DISPL: Keeps track of the current and cumulative displacements throughout successive runs.

STRESP: Calculates stresses in a plane solid.

STRESX: Calculates stresses in an axisymmetric solid.

PLOT2: Plots the deformed mesh with stresses at the center of each element, for any iteration.

RCSGTH: Checks stresses against failure criteria in the solids and recomputes current modulus and Poisson's ratio if needed. Calculates factor of safety against tensile and shear failure.

PLOT3: Plots the mesh at the end of the last iteration, without stresses.

JTSTR: Calculates joint element relative displacements and stresses, without dilation effects. Plane and axisymmetric cases.

DLTSIG: Calculates the increase in normal joint stress, the current dilation angle and the new shear stiffness of dilatant joints.

JTSGTH: Checks stresses against failure criteria in the joints and recomputes current shear and normal stiffnesses if required. Calculates factors of safety against shear and tensile failure of joints.

## 5. INPUT PREPARATION

### 5.1 Input Format

Consistent units must be used. The current code version requires use of SI quantities.

A. Start Card: Punch START in columns 1-5 as the first card for any problem.

B. File Card: (LLNL specific) Output filing code (3A10)

C. Identification Card: (12A6)

Columns 1-72 Caption of problem

D. Control Card: (2I5, I3, I2, I5, 2E10.3, 9I4)

1 - 5 Number of nodal points (500 maximum), NUMNP

6-10 Number of elements (400 maximum), NUMEL

11-13 Number of different materials (12 maximum) including joint materials, NUMMAT

14-15 Joint stiffness number:

- 0 - joint without rotation stiffness; line integration.
- 1 - joint without rotation stiffness; 1-point integration.
- 2 - joint with rotation stiffness.

16-20 Number of boundary pressure cards (100 maximum), NUMPC

21-30 Acceleration in X-direction, ACCELX

31-40 Acceleration in Y-direction (gravity is input as positive in the negative Y-direction), ACCELY

41-44 Number of iterations in the run.

45-48 Residual stress code, RSTRS

0 - no residual stresses are read.

1 - residual stresses will be read. Always the case in a RESTART.

49-52 Joint cut-off number; all materials with higher numbers are joints, NSHELL

52-56 Print and plot option, IPLOT

0 - if no results will be plotted.

1 - if in any iteration a plot is desired.

57-60 Restart option, IPUN

0 - if it is a new problem and the results will not be punched

1 - if it is a new problem and the results will be punched

2 - if it is a RESTART. The results will also be punched.

61-64 Dilatancy option, IDLT

0 - if there is no dilatant joint in the mesh

1 - if any joint in the mesh is dilatant

65-68 Number of joint elements, NJTMAX. When numbering elements, all the joints must be numbered first, starting at 1.

69-72 Analysis option

0 - plane analysis; Navier-Coulomb criterion in solids

1 - axisymmetric; Navier-Coulomb criterion in solids

2 - axisymmetric; Murrell criterion in solids

73-76 Material option

0 - Isotropic solids

1 - Transversely isotropic solids

If any material is anisotropic, use option 1.

E. Plot Option Card:

Defines whether a plot is produced in a given iteration (40I2). There can be up to 40 iterations.

1 - no plot will be produced

2 - a plot of the structure with stresses will be produced.

This card must be present. It is punched with "ones" if no plot is desired on card D. Do not request a plot of iteration 1, when IDLT = 1.

F. <u>Plot Scale Card</u>: (8E10.2) Only if a plot is desired at any time (IPLOT = 1 in card D)

1 -10 ROO. SCALE 1.

11-20 ZOO. SCALE 2.

21-30 Mesh Scale Factor; multiplies the prototype dimensions, whatever the units, to get the plot dimensions in inches. SCALE 3.

31-40 Prototype displacement corresponding to a displacement of 1 inch on the plot. SCALE 4

41-50 Punch 1.00E00. SCALE 5

51-60 Prototype stress corresponding to a 1 inch line on the plot. SCALE 6

61-70 Punch 1.00E00. SCALE 7

70-80 Larger of x or y dimension of the structure.

<u>Notes on Plotting</u>

1. The user determines the size of the sum of left and right margins on each plot frame by specifying SCALE 8, which is = prototype length * SCALE 3 + margins.
2. The stresses are plotted in all elements except joints and elements with material number = NSHELL. This material number could be reserved for the steel of bolts, for example, where the stresses will be very high compared to those in the rock.
3. When nodes on the mesh have negative coordinates, it is desirable to shift the plot origin to a new position (ROO, ZOO). ROO, ZOO should be positive and equal respectively to the absolute values of the most negative coordinates r and z (or x & y) in the mesh.
4. In each run where plots are produced the plot output will be:
   (a) The starting mesh undeformed, or deformed in a RESTART, at SCALE 3. No magnification of the displacements.
   (b) For each iteration where requested (card F), stresses at the center of each element in the deformed mesh of this iteration. Current displacements are included but not magnified.
   (c) The deformed mesh at the end of the run, with the displacements magnified by SCALE 5/SCALE 4.

Note that with IPLOT=1, even if no stress plot is requested in any of the iterations, the final mesh still will be produced. The initial mesh will not be produced in any RESTART run.

5. This program can run multiple problems, except when plotting is used. In this case separate runs must be made for the different problems.

## G. Material Property Cards

The following group of cards must be supplied for each different solid material and joint material. Unless otherwise noted all input quantities are positive.

### Solid Materials

1st Card (2I5, E10.2, 5A10)

1-5 Material identification number; up to 12 materials, including joint materials, can be specified.

6-10 Material flag, to simplify input to RESTART problems.

- 0 - Read stresses and moduli from RESTART deck, which can be obtained automatically in previous run if IPUN = 1 or 2.
- 1 - Read stresses from RESTART deck; read moduli from original material cards.
- 2 - Set stresses equal to zero; read moduli from original material cards.

A discussion of these codes is found in the notes on Restarts, paragraph 5.2.

10-20 Mass density of materials = unit weight/acceleration of gravity

21-70 Name of material type, if desired.

2nd Card (5E10.2)

1-10 Residual friction angle, $\phi_r$ (degrees)

11-20 Tensile strength, $\sigma_{t1}$; must not be zero; can be very small.

21-30 Tensile strength, $\sigma_{t3}$; must not be zero; can be very small.

31-40 Peak cohesion, c

41-50 Peak friction angle, $\phi_p$ (degrees)

3rd Card (5E10.2)

1-10 $E_1$ modulus

11-20 $E_2$ modulus

21-30 $\nu_1$ Poisson's ratio

31-40 $\nu_2$ Poisson's ratio

41-50 G shear modulus.

For isotropic materials leave $E_2$, $\nu_2$ and G blank.

Note: If a Murrell criterion is used for the solids, the tensile strength must be set at a value no greater than $\sigma_t = \frac{c}{6} \times \tan (45^o + \frac{\phi_p}{2})$ which corresponds to a ratio of uniaxial to tensile strength = 12.

Joint Materials

1st Card (2I5, E10.2, 5A10)

1-5 Joint material number

6-10 Material flag; same conventions as for solids.

11-20 Blank

21-70 Name of joint type, if desired.

2nd Card (8E10.2)

1-10 Normal stiffness, $(F/L^3)$

11-20 Tangential stiffness, $(F/L^3)$

21-30 Peak cohesion (zero for non cemented joints)

31-40 $C_p$ back intercept of peak envelope (Fig. 8) It is zero for a nondilatant joint.

41-50 Maximum closure of joint; input as negative quantity.

51-60 Residual cohesion must be zero (except for excavated joints as described in paragraph 5.2)

61-70 Residual friction angle

71-80 Tensile strength of joint.

3rd Card (2E10.2) Required, whether IDLT = 0 or not.

1-10 Initial dilation angle of the joint in degrees. This angle will be adjusted internally in the program according to the current normal stress on the joint. The program will print this current dilation angle (DLNGL) for each joint, at the end of each iteration. In this program, the joints are taken as bi-dilatant. The angle is always $\geq 0$.

11-20 Maximum normal stress on the joint beyond which the joint cannot dilate. This number must be input as a negative (compressive) stress, and it cannot be zero. Use -1.00E10 for steel joints, excavated joints, and others for which the dilation angle is assumed to be zero.

H. Nodal Point Cards: (2I5, 4E10.3)

One card for each nodal point. Joint elements are obtained by double rows of nodal points at the same coordinates.

1-5 Nodal point number.

6-10 Number which indicates if displacements or forces are to be specified.

If the number in column 10 is

0: XR is the specified X-load and XZ is the specified Y-load.

1: XR is the specified X-displacement and XZ is the specified Y-load.

2: XR is the specified X-load and XZ is the specified Y-displacement.

3: XR is the specified X-displacement and XZ is the specified Y-displacement.

11-20 X-ordinate.

21-30 Y-ordinate.

31-40 XR

41-50 XZ

If nodal cards are omitted, the program automatically generates (p-1) nodes at equal intervals between the last node read, n, and the new one read, n+p. These nodes are not constrained or loaded (zeros in columns 10, 40, and 50).

I. Second Deck of Nodal Cards (2I5, 4F10.4)

In a RESTART run, the 2nd deck of nodal cards must be read. It shows the current coordinates of the nodes. It is punched automatically from the previous run of the problem, if IPUN = 1 or 2.

J. <u>Element Cards</u>: (6I5)

<u>Joint Elements</u>

All joint elements in the mesh must be numbered first, from 1 to NJTMAX; then, the solid elements are numbered.

Nodal points must be numbered I, J, K, L counter clockwise proceeding along length of joint from I to J and along length from K to L. Nodal point pairs (I, L) and (J, K) have different numbers but identical coordinates.

<u>Solid Elements</u>

One card for each element. For a right hand coordinate system, order nodal points counter-clockwise around the element.

In any solid or joint element, the maximum difference between nodal point numbers must be less than or equal to (MBMAX-2)/2. Here MBMAX = 100.

| | |
|---|---|
| 1-5 | Element number |
| 6-10 | Nodal point I |
| 11-15 | Nodal point J |
| 16-20 | Nodal point K |
| 21-25 | Nodal point L |
| 26-30 | Material identification number. |

Element cards must be in numbered sequence. If element cards are omitted, the program automatically generates the omitted information by incrementing by one the preceding I, J, K, and L. The material identification code for the generated cards is set equal to the value in the last card. The last element card must always be supplied.

Triangular elements are also permissible. They are identified by repeating the last nodal point number (i.e., I, J, K, K).

K. <u>Pressure Cards</u>: (2I5, 2E10.2)

One card for each side of each solid element, upon which a normal pressure is applied.

| | |
|---|---|
| 1-5 | Nodal point I |
| 6-10 | Nodal point J |
| 11-20 | Normal pressure at I |
| 21-30 | Normal pressure at J |

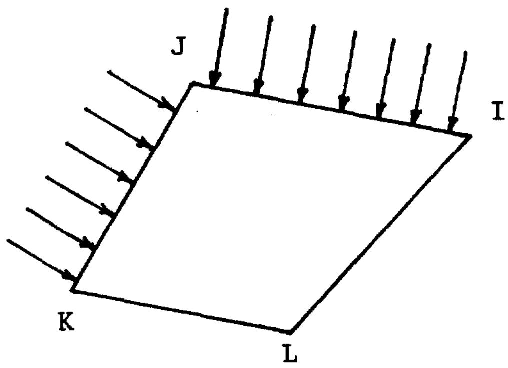


2 Cards: (I,J), and (J,K)

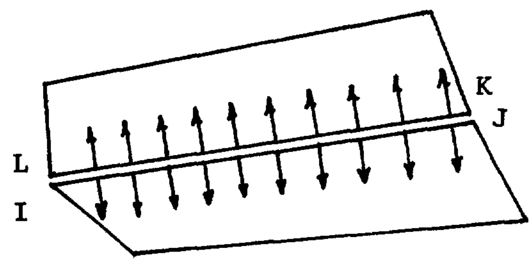


Water pressure in the joint:
2 Cards: (J,I) and (L,K)

Figure 10: Convention for Input of Boundary Pressures

As shown above, the element must be on the left as one progresses from I to J. Surface compression (tension) is input as a positive (negative) pressure. Joints can be placed on boundaries.

L. Residual Stress Cards: (I3, 4E9.2)

If the residual stress code, RSTRS, on the control card is not equal to 0, one card must be supplied for each element, with the following information:

1-3 Element number

4-12 Plane analysis: major principal stress (smallest compression) in solids, or X stress in joints.
Axisymmetric analysis: R stress in solids and joints.

13-21 Plane analysis: minor principal stress (largest compression) in solids, or Y stress in joints
Axisymmetric analysis: Z stress in solids and joints.

22-30 Plane analysis: angle (degrees), positive from X direction to direction of major principal stress.
Not applicable to joints (leave blank).
Axisymmetric analysis: θ stress in solid elements. Blank for joints.

31-39 Plane analysis: blank for solids and joints.

Axisymmetric analysis: RZ stress in solid elements. Blank in joints. The sign convention is: tension positive.

If the structure is loaded initially by gravity or boundary pressure cards, these initial stress cards are not needed. In the RESTART option, the residual stress deck of cards is punched from the previous run and placed here in lieu of the original residual stress deck. Note that whereas principal stresses are input originally, the punched deck for RESTART contains the x,y, and xy stresses instead. All stress transformations are done internally. This deck also contains the shear and normal joint stiffnesses, and the solid moduli calculated at the end of the last iteration performed.

M. Stop Card:

This program can run several problems in a sequence. The last card of the last data deck must be STOP punched in columns 1-4.

In summary, for the very first run on a problem, a typical sequence of cards would be: cards A, B, C, D, E, (optional), F, G, H, J, K, (optional), L (optional), M No cards I.

## 5.2 Notes on Restarts

In many cases, the analysis of geological engineering problems entails the simulation of sequential excavation or sequential construction. For example, if a tunnel is excavated by the heading and bench method, the problem will be analyzed in three steps, called "runs":

run 1 - no tunnel; obtain equilibrium in the rock mass

run 2 - RESTART: excavate the tunnel heading; obtain equilibrium (if the prototype proves to be stable)

run 3 - RESTART: excavate the bench.

At the beginning of each RESTART there is an opportunity to introduce modifications in the structure; ex: lining, bolting. One may also reassign material properties; ex: some rock will be blast damaged in the next excavation step and will be reassigned a lower modulus, as well as reduced strength, at the outset of the calculation. Or a solid or joint element will be excavated and its material number must be changed to that of excavated rock or joint.

To facilitate the RESTARTS, one uses the material flag mentioned above (Cards
Code 1 is used for elements in which one wants to specify a new material at the beginning of a RESTART calculation. Such is the case for rock which is to be blast damaged in the vicinity of a new underground excavation. The stresses start where they left in the previous calculation, before blasting, but the modulus is readjusted by the user before the new run.
Code 2 is used for excavated materials, which are defined in the original material numbers (e.g., excavated rock, excavated joint).
Code 0 is for all the other elements which are subject to a RESTART.

Additional precautions must be taken as follows:

1. For the solids and the joints, the material will be very soft but very strong so that its initial modulus or stiffnesses will not be modified by the program.
2. For solids and joints which are excavated, the following properties should be assigned:
   peak cohesion = residual cohesion = tensile strength = a very high number.
   peak friction = residual friction = 0.

A typical deck set up for a RESTART will be: cards A, B, C, D, E (optional), F, G, H, I, J, K, (optional), L, M.

## 5.3 Sample Input

Two sample input decks are shown to illustrate the above instructions. The analysis is that of Station 2+83 in the Spent Fuel Test Tunnels which were excavated in three steps (paragraph 7.11). We show the input to run 1, in which the mesh was gravity loaded in the vertical direction and loaded by boundary pressure cards in the horizontal direction. This calculation was nondilatant. We also show the input to run 2, in which the two side drifts were excavated. It was a dilatant calculation. Plots were requested in both calculations.

Input to SFTC - Station 2+83 - Run 1

```
START
BOX U75
SFTC MINE-BY. STATION 2+83. RUN 1. GRAVITY LOADING. NO EXCAVATION. NO DILATION
  381   382   6 0    39           0.          9.81    2    0    3    1    1    0  85    0    0
 2 2
      2.          2.         .15        .25          1.      1.E+08         1.          12.
   1    0       2650.    UNDAMAGED ROCK
     45.     1.0E+07    1.0E+07    7.0E+06         60.
  3.0E+10    3.0E+10        .25        .25     1.2E+10
   2    1       2600.  EXPLOSIVE DAMAGED ROCK
     45.     2.0E+06    2.0E+06    3.5E+06         45.
  1.0E+10    1.0E+10        .35        .35    3.70E+09
   3    2          1.    EXCAVATED ROCK
      0.     1.0E+10    1.0E+10    1.0E+10          0.
  1.0E+04    1.0E+04        .25        .25       4000.
   4    0          0.     ROCK JOINT TYPE 1
  1.0E+11    2.7E+09         0.         0.   -2.0E-03          0.        40.          0.
      0.   -1.00E+10
   5    1          0.    ROCK JOINT TYPE 2
  1.0E+11    2.7E+09         0.         0.   -2.0E-03          0.        25.          0.
      0.   -1.00E+10
   6    2          0.    EXCAVATED JOINT
  1.0E+03    1.0E+02    1.0E+10         0.   2.0E+02    1.0E+10          0.     1.0E+10
      0.   -1.00E+10
```

```
   1     2 0.        0.        0.
   2     2 13.       0.        0.
   3     3 25.       0.        0.
   4     2 33.4      0.        0.
   5     2 33.4      0.        0.

 377     0 12.       70.       0.
 378     0 25.       70.       0.
 379     0 34.75     70.       0.
 380     0 43.       70.       0.
 381     0 50.       70.       0.
```

Nodes

```
   1     5    14    13     4     4
   2    14    27    26    13     4
   3    27    46    45    26     4
   4    46    66    65    45     4
   5    66    93    92    65     4

 378   369   370   379   378     1
 379   370   371   380   379     1
 380   371   372   381   380     1
 381   134   135   174   174     1
 382    94    95   137   137     1
```

Elements

```
 381   380 9.686E+06 9.686E+06
 380   379 9.686E+06 9.686E+06
 379   378 9.686E+06 9.686E+06
 378   377 9.686E+06 9.686E+06
 377   376 9.686E+06 9.686E+06

  80    56 1.304E+07 1.310E+07
  56    36 1.310E+07 1.321E+07
  36    21 1.321E+07 1.340E+07
  21    10 1.340E+07 1.356E+07
  10     1 1.356E+07 1.381E+07
STOP
```

Boundary Pressures

Input to SFTC - Station 2+83 - Run 2

```
START
BOX U75
SFTC MINE-BY. STATION 2+83. RUN 2. EXCAVATE SIDE DRIFTS. DILATANT
  381   382   6 0    39          0.        9.81    4    1    3    1    2    1   85    0    0
 2 2 2 2
        2.          2.         .15         .25          1.      1.E+08          1.          12.
   1    0        2650.    UNDAMAGED ROCK
      45.    1.0E+07    1.0E+07    7.0E+06          60.
  3.0E+10    3.0E+10        .25         .25    1.2E+10
   2    1        2600.  EXPLOSIVE DAMAGED ROCK
      45.    2.0E+06    2.0E+06    3.5E+06          45.
  1.0E+10    1.0E+10        .35         .35   3.70E+09
   3    2           1.    EXCAVATED ROCK
       0.    1.0E+10    1.0E+10    1.0E+10           0.
  1.0E+04    1.0E+04        .25         .25        4000.
   4    0            0.     ROCK JOINT TYPE 1
  1.0E+11     2.7E+09         0.          0.   -2.0E-03          0.         40.          0.
      10.  -7.00E+07
   5    1           0.    ROCK JOINT TYPE 2
  1.0E+11     2.7E+09         0.          0.   -2.0E-03          0.         25.          0.
      10.  -7.00E+07
   6    2           0.    EXCAVATED JOINT
  1.0E+03     1.0E+02    1.0E+10          0.    2.0E+02    1.0E+10          0.     1.0E+10
       0.  -1.00E+10
```

Original Nodal Coordinates

```
   1      2 0.          0.          0.
   2      2 13.         0.          0.
   3      3 25.         0.          0.
   4      2 33.4        0.          0.
   5      2 33.4        0.          0.

 377      0 12.         70.         0.
 378      0 25.         70.         0.
 379      0 34.75       70.         0.
 380      0 43.         70.         0.
 381      0 50.         70.         0.
```

Current Nodal Coordinates

```
   1      2 9.164E-03 0.          0.          0.
   2      2 1.300E+01 0.          0.          0.
   3      3 2.500E+01 0.          0.          0.
   4      2 3.340E+01 0.          0.          0.
   5      2 3.340E+01 0.          0.          0.

 377      0 1.201E+01 6.999E+01 0.          0.
 378      0 2.501E+01 6.999E+01 0.          0.
 379      0 3.475E+01 6.999E+01 0.          0.
 380      0 4.300E+01 6.999E+01 0.          0.
 381      0 5.000E+01 6.999E+01 0.          0.
```

Elements

```
   1     5    14    13     4     4
   2    14    27    26    13     4
   3    27    46    45    26     4
   4    46    66    65    45     4
   5    66    93    92    65     4
```

(explosively damaged elements)

```
 183   110   113   112   111     2
 184   113   116   114   112     2
 185   115   117   156   155     2
```

(excavated elements)

```
 186   111   112   152   148     3
 187   112   114   152   152     3
 188   115   155   153   153     3

 378   369   370   379   378     1
 379   370   371   380   379     1
 380   371   372   381   380     1
 381   134   135   174   174     1
 382    94    95   137   137     1
```

```
381   380 9.686E+06 9.686E+06
380   379 9.686E+06 9.686E+06
379   378 9.686E+06 9.686E+06
378   377 9.686E+06 9.686E+06
377   3[illegible] 9.686E+06 9.686E+06
```

Boundary Pressures

```
 56    36 1.310E+07 1.321E+07
 36    21 1.321E+07 1.340E+07
 21    10 1.340E+07 1.356E+07
 10     1 1.356E+07 1.381E+07
```

```
86-1.40E+07-7.51E+06 2.12E+05 0.         0.         0.
86 3.00E+10 3.00E+10 2.50E-01 2.50E-01 1.20E+10
87-1.50E+07-1.03E+07 5.96E+05 0.         0.         0.
87 3.00E+10 3.00E+10 2.50E-01 2.50E-01 1.20E+10

382 3.00E+10 3.00E+10 2.50E-01 2.50E-01 1.20E+10
```

Restart Stresses and Current Properties of Solid Elements

```
 1-1.41E+07-9.17E+05 0.        0.        2.70E+09 1.00E+11
 2-1.42E+07-1.78E+06 0.        0.        2.70E+09 1.00E+11
 3-1.43E+07-2.24E+06 0.        0.        2.70E+09 1.00E+11
 4-1.32E+07-2.67E+06 0.        0.        2.70E+09 1.00E+11
 5-1.69E+07-2.85E+06 0.        0.        2.70E+09 1.00E+11

81-1.43E+07-2.86E+06 0.        0.        2.70E+09 1.00E+11
82-9.26E+06-2.59E+06 0.        0.        2.70E+09 1.00E+11
83-1.29E+07-2.90E+06 0.        0.        2.70E+09 1.00E+11
84-1.24E+07-2.95E+06 0.        0.        2.70E+09 1.00E+11
85-1.18E+07-2.77E+06 0.        0.        2.70E+09 1.00E+11
STOP
```

Restart Stresses and Current Stiffnesses of Joint Elements

# 6. OUTPUT

## 6.1 Output Information

At the beginning of a run the program prints the following:

- Control card information
- Material, node, and element information; original nodal coordinates as well as current coordinates are given in a RESTART
- Element stresses to start the new run (omitted if initial run with gravity loading)
- Current solid and joint stiffnesses
- Current KNEFF, if dilatant analysis

At the end of the run:

- Current nodal displacements
- Cumulative nodal displacements, if a RESTART
- Stresses at the center of solid elements
- Tensile (TENFAC) and shear (SHFAC) factors of safety for the solids. Particular values are:

| | | |
|---|---|---|
| SHFAC | = 1.0 | if shear failure has occurred |
| SHFAC | = 0. | if tensile failure has occurred |
| TENFAC | = 1.0 | if tensile failure has occurred |
| TENFAC | = $10^{10}$ | if both principal stresses are compressive |

- Current modulus of the solids
- Shear and normal stresses in the joints
- Shear and normal relative displacements of the joints
- Current shear and normal joint stiffnesses, and joint dilation angle
- Shear factor of safety of the joints (SHFAC)

## 6.2 Sample Output

We show both outputs of the two runs for which we gave the inputs in paragraph 5.3. One can note that the stresses and material properties at the end of run 1 are the same as those at the beginning of run 2 except for changes made by the user to excavate new elements, or soften other elements.

Output to SFTC - Station 2+83 - Run 1

```
SFTC MINE-BY. STATION 2+83. RUN 1. GRAVITY LOADING. NO EXCAVATION. NO DILATION

                PLANE STRAIN ANALYSIS - ISOTROPIC SOLIDS
              THE 1 AND 2 DIRECTIONS ARE X AND Y RESPECTIVELY

NUMBER OF NODAL POINTS------381
NUMBER OF ELEMENTS----------382
NUMBER OF JOINT ELEMENTS---- 85
NUMBER OF MATERIALS---------  6
NUMBER OF PRESSURE CARDS---- 39
ACCELERATION, DIRECTION 1---  0.
ACCELERATION, DIRECTION 2---  9.810
NUMBER OF ITERATIONS--------  2
HIGHEST SOLID MATERIAL------  3
PLOT OPTION-----------------  1
PUNCH OPTION----------------  1
DILATION OPTION-------------  0
JOINT STIFFNESS OPTION------  0
OUTPUT SCHEME---------------  2 2

ORIGIN CHANGE   RO =   2.00    ZO =   2.00
MESH SCALE FACTOR = 0.150
ONE INCH CORRESPONDS TO A DISPLACEMENT OF  2.50E-01
ONE INCH CORRESPONDS TO A STRESS OF    1.00E+08
LENGTH OF EACH PLOT FRAME =  12.00 INCHES


MATERIAL NO =  1   .   UNDAMAGED ROCK
    MASS DENSITY        =   2.65E+01          NEW MATERIAL FLAG =          0
    RESIDUAL FRICTION   =   4.50E+01          TENSILE STRENGTH  =   1.00E+07
    PEAK COHESION       =   7.00E+06          PEAK FRICTION     =   6.00E+01
    MODULUS             =   3.00E+10          POISSON RATIO     =   2.50E-01
```

materials 2 to 5 omitted

```
MATERIAL NO =  6   .   EXCAVATED JOINT
    NEW MATERIAL FLAG       =          2        NORMAL STIFFNESS   =   1.00E+03
    RESIDUAL FRICTION       =   0.              SHEAR STIFFNESS    =   1.00E+02
    TENSILE STRENGTH        =   1.00E+10        MAXIMUM CLOSURE    =   2.00E+02
    CPSTAR                  =   0.              PEAK COHESION      =   1.00E+10
    INITIAL DILATION ANGLE  =   0.              RESIDUAL COHESION  =   1.00E+10
    CRITICAL NORMAL STRESS  =  -1.00E+10
```

| NODAL POINT | TYPE | R-ORIGINAL | Z-ORIGINAL | R-LOAD OR DISPLACEMENT | Z-LOAD OR DISPLACEMENT |
|---|---|---|---|---|---|
| 1 | 2 | 0. | 0. | 0. | 0. |
| 2 | 2 | 13.000 | 0. | 0. | 0. |
| 3 | 3 | 25.000 | 0. | 0. | 0. |
| 4 | 2 | 33.400 | 0. | 0. | 0. |
| 5 | 2 | 33.400 | 0. | 0. | 0. |
| | | | | | |
| 377 | 0 | 12.000 | 70.000 | 0. | 0. |
| 378 | 0 | 25.000 | 70.000 | 0. | 0. |
| 379 | 0 | 34.750 | 70.000 | 0. | 0. |
| 380 | 0 | 43.000 | 70.000 | 0. | 0. |
| 381 | 0 | 50.000 | 70.000 | 0. | 0. |

| ELEMENT | I | J | K | L | MATERIAL |
|---|---|---|---|---|---|
| 1 | 5 | 14 | 13 | 4 | 4 |
| 2 | 14 | 27 | 26 | 13 | 4 |
| 3 | 27 | 46 | 45 | 26 | 4 |
| 4 | 46 | 66 | 65 | 45 | 4 |
| 5 | 66 | 93 | 92 | 65 | 4 |
| | | | | | |
| 378 | 369 | 370 | 379 | 378 | 1 |
| 379 | 370 | 371 | 380 | 379 | 1 |
| 380 | 371 | 372 | 381 | 380 | 1 |
| 381 | 134 | 135 | 174 | 174 | 1 |
| 382 | 94 | 95 | 137 | 137 | 1 |

Reprint of Input Data

BANDWIDTH = 92

PRESSURE BOUNDARY CONDITIONS

| I | J | PRESS. I | PRESS. J |
|---|---|---|---|
| 381 | 380 | 9.69E+06 | 9.69E+06 |
| 380 | 379 | 9.69E+06 | 9.69E+06 |
| 379 | 378 | 9.69E+06 | 9.69E+06 |
| | | | |
| 36 | [illegible] | 1.32E+07 | 1.34E+07 |
| [illegible] | [illegible] | 1.34E+07 | 1.36E+07 |
| 1[illegible] | [illegible] | 1.36E+07 | 1.38E+07 |

ITERATION NUMBER 1

Results of First Calculation Start Here

| NODE | CURRENT R-DISPL | CURRENT Z-DISPL |
|---|---|---|
| 1 | 9.164E-03 | 0. |
| 2 | 4.466E-03 | 0. |
| 3 | 0. | 0. |
| 4 | -2.777E-03 | 0. |
| 5 | -2.950E-03 | 0. |
| | | |
| 377 | 8.323E-03 | -6.584E-03 |
| 378 | 5.207E-03 | -7.439E-03 |
| 379 | 2.865E-03 | -8.744E-03 |
| 380 | 8.401E-04 | -1.025E-02 |
| 381 | -1.005E-03 | -1.161E-02 |

| ELEMENT | R | Z | R-STRESS | Z-STRESS | RZ-STRESS | MAX-STRESS | MIN-STRESS | ANGLE | TENFAC | SHFAC | NEXT EMOD |
|---|---|---|---|---|---|---|---|---|---|---|---|
| 86 | 6.50 | 4.10 | -1.40E+07 | -7.54E+06 | 2.14E+05 | -7.53E+06 | -1.40E+07 | 88.26 | 1.00E+10 | 1.12E+01 | 3.00E+10 |
| 87 | 19.00 | 4.10 | -1.51E+07 | -1.03E+07 | 5.95E+05 | -1.03E+07 | -1.51E+07 | 83.07 | 1.00E+10 | 1.29E+01 | 3.00E+10 |
| 88 | 28.17 | 4.10 | -1.46E+07 | -1.16E+07 | 6.61E+05 | -1.14E+07 | -1.48E+07 | 78.45 | 1.00E+10 | 1.43E+01 | 3.00E+10 |
| 89 | 32.13 | 4.10 | -1.47E+07 | -1.08E+07 | 1.01E+05 | -1.08E+07 | -1.47E+07 | 88.69 | 1.00E+10 | 1.38E+01 | 3.00E+10 |
| 90 | 39.70 | 4.10 | -1.45E+07 | -1.03E+07 | -1.29E+05 | -1.03E+07 | -1.45E+07 | -88.41 | 1.00E+10 | 1.35E+01 | 3.00E+10 |
| 91 | 47.67 | 5.47 | -1.59E+07 | -9.41E+06 | -9.21E+05 | -9.28E+06 | -1.60E+07 | -82.22 | 1.00E+10 | 1.13E+01 | 3.00E+10 |
| 92 | 5.75 | 10.60 | -1.40E+07 | -7.75E+06 | 6.64E+05 | -7.68E+06 | -1.41E+07 | 84.14 | 1.00E+10 | 1.13E+01 | 3.00E+10 |
| 93 | 12.00 | 11.40 | -1.49E+07 | -9.32E+06 | 8.92E+05 | -9.18E+06 | -1.51E+07 | 81.32 | 1.00E+10 | 1.20E+01 | 3.00E+10 |
| 94 | 14.50 | 11.40 | -1.50E+07 | -9.34E+06 | 9.45E+05 | -9.18E+06 | -1.51E+07 | 80.88 | 1.00E+10 | 1.19E+01 | 3.00E+10 |
| 95 | 19.50 | 10.60 | -1.49E+07 | -1.02E+07 | 8.09E+05 | -1.01E+07 | -1.51E+07 | 80.68 | 1.00E+10 | 1.28E+01 | 3.00E+10 |
| 96 | 25.95 | 10.60 | -1.51E+07 | -1.12E+07 | 3.95E+05 | -1.11E+07 | -1.51E+07 | 84.45 | 1.00E+10 | 1.37E+01 | 3.00E+10 |
| 377 | 18.50 | 63.00 | -1.22E+07 | -9.77E+06 | -2.15E+04 | -9.77E+06 | -1.22E+07 | -89.65 | 1.00E+10 | 1.55E+01 | 3.00E+10 |
| 378 | 29.88 | 63.00 | -1.22E+07 | -9.68E+06 | -2.77E+04 | -9.68E+06 | -1.22E+07 | -89.52 | 1.00E+10 | 1.54E+01 | 3.00E+10 |
| 379 | 38.88 | 63.00 | -1.20E+07 | -9.77E+06 | -1.16E+04 | -9.77E+06 | -1.20E+07 | -89.86 | 1.00E+10 | 1.57E+01 | 3.00E+10 |
| 380 | 46.50 | 63.00 | -1.17E+07 | -9.56E+06 | -1.98E+05 | -9.54E+06 | -1.17E+07 | -84.94 | 1.00E+10 | 1.58E+01 | 3.00E+10 |
| 381 | 19.73 | 27.03 | -1.59E+07 | -1.11E+07 | 1.28E+06 | -1.08E+07 | -1.63E+07 | 76.12 | 1.00E+10 | 1.25E+01 | 3.00E+10 |
| 382 | 22.00 | 25.25 | -1.58E+07 | -8.92E+06 | 5.53E+05 | -8.88E+06 | -1.58E+07 | 85.57 | 1.00E+10 | 1.11E+01 | 3.00E+10 |

Stresses, Safety Factors and Modulus of Solids, After the First Iteration in Run 1

| ELEMENT | R | Z | NORMAL STRESS | TANGENT STRESS | NORMAL DISPL | TANGENT DISPL | NEXT KN | NEXT KS | SHFAC | DLNGL |
|---|---|---|---|---|---|---|---|---|---|---|
| 1 | 31.35 | 4.10 | -1.41E+07 | -9.17E+05 | -1.41E-04 | -3.40E-04 | 1.00E+11 | 2.70E+09 | 1.29E+01 | 0. |
| 2 | 28.15 | 10.60 | -1.42E+07 | -1.78E+06 | -1.42E-04 | -6.58E-04 | 1.00E+11 | 2.70E+09 | 6.69E+00 | 0. |
| 3 | 25.50 | 16.00 | -1.43E+07 | -2.23E+06 | -1.43E-04 | -8.26E-04 | 1.00E+11 | 2.70E+09 | 5.39E+00 | 0. |
| 4 | 23.10 | 20.75 | -1.32E+07 | -2.66E+06 | -1.32E-04 | -9.86E-04 | 1.00E+11 | 2.70E+09 | 4.15E+00 | 0. |
| 5 | 21.78 | 23.40 | -1.71E+07 | -2.85E+06 | -1.71E-04 | -1.06E-03 | 1.00E+11 | 2.70E+09 | 5.03E+00 | 0. |
| 6 | 20.78 | 25.40 | -9.23E+06 | -2.96E+06 | -9.23E-05 | -1.10E-03 | 1.00E+11 | 2.70E+09 | 2.62E+00 | 0. |
| 81 | 23.95 | 36.00 | -1.42E+07 | -2.84E+06 | -1.42E-04 | -1.05E-03 | 1.00E+11 | 2.70E+09 | 4.20E+00 | 0. |
| 82 | 20.63 | 38.80 | -9.20E+06 | -2.58E+06 | -9.20E-05 | -9.55E-04 | 1.00E+11 | 2.70E+09 | 2.99E+00 | 0. |
| 83 | 15.18 | 43.30 | -1.29E+07 | -2.90E+06 | -1.29E-04 | -1.07E-03 | 1.00E+11 | 2.70E+09 | 3.73E+00 | 0. |
| 84 | 10.75 | 47.00 | -1.24E+07 | -2.95E+06 | -1.24E-04 | -1.09E-03 | 1.00E+11 | 2.70E+09 | 3.54E+00 | 0. |
| 85 | 4.75 | 52.00 | -1.18E+07 | -2.76E+06 | -1.18E-04 | -1.02E-03 | 1.00E+11 | 2.70E+09 | 3.60E+00 | 0. |

Corresponding Information for the Joints

ITERATION NUMBER 2

| NODE | CURRENT R-DISPL | CURRENT Z-DISPL |
|---|---|---|
| 1 | 9.164E-03 | 0. |
| 2 | 4.463E-03 | 0. |
| 3 | 0. | 0. |
| 4 | -2.775E-03 | 0. |
| 5 | -2.948E-03 | 0. |
| 377 | 8.424E-03 | -6.548E-03 |
| 378 | 5.311E-03 | -7.422E-03 |
| 379 | 2.971E-03 | -8.746E-03 |
| 380 | 9.474E-04 | -1.027E-02 |
| 381 | -8.974E-04 | -1.164E-02 |

| NODE | CUMUL R-DISPL | CUMUL Z-DISPL |
|---|---|---|
| 1 | 9.164E-03 | 0. |
| 2 | 4.463E-03 | 0. |
| 3 | 0. | 0. |
| 4 | -2.775E-03 | 0 |
| 5 | -2.948E-03 | 0. |
| 377 | 8.424E-03 | -6.548E-03 |
| 378 | 5.311E-03 | -7.422E-03 |
| 379 | 2.971E-03 | -8.746E-03 |
| 380 | 9.474E-04 | -1.027E-02 |
| 381 | -8.974E-04 | -1.164E-02 |

Iteration 2 is the last one in Run 1.

In the case of Run 1, the cumulative displacements are the same as the current ones, because there was no restart from a previously deformed configuration.

Final solid and joint stresses would be printed here, as on the previous page.

Output to SFTC - Station 2+83 - Run 2

SFTC MINE-BY. STATION 2+83. RUN 2. EXCAVATE SIDE DRIFTS. DILATANT

PLANE STRAIN ANALYSIS - ISOTROPIC SOLIDS
THE 1 AND 2 DIRECTIONS ARE X AND Y RESPECTIVELY

NUMBER OF NODAL POINTS------381
NUMBER OF ELEMENTS----------382
NUMBER OF JOINT ELEMENTS---- 85
NUMBER OF MATERIALS--------- 6
NUMBER OF PRESSURE CARDS---- 39
ACCELERATION, DIRECTION 1--- 0.
ACCELERATION, DIRECTION 2--- 9.810
NUMBER OF ITERATIONS-------- 4
HIGHEST SOLID MATERIAL------ 3
PLOT OPTION----------------- 1
PUNCH OPTION---------------- 2
DILATION OPTION------------- 1
JOINT STIFFNESS OPTION------ 0
OUTPUT SCHEME--------------- 2 2 2 2

ORIGIN CHANGE RO = 2.00 ZO = 2.00
MESH SCALE FACTOR = 0.150
ONE INCH CORRESPONDS TO A DISPLACEMENT OF 2.50E-01
ONE INCH CORRESPONDS TO A STRESS OF 1.00E+08
LENGTH OF EACH PLOT FRAME = 12.00 INCHES

MATERIAL NO = 1 . UNDAMAGED ROCK

| | | | |
|---|---|---|---|
| MASS DENSITY = | 2.65E+01 | NEW MATERIAL FLAG = | 0 |
| RESIDUAL FRICTION = | 4.50E+01 | TENSILE STRENGTH = | 1.00E+07 |
| PEAK COHESION = | 7.00E+06 | PEAK FRICTION = | 6.00E+01 |
| MODULUS = | 3.00E+10 | POISSON RATIO = | 2.50E-01 |

MATERIAL NO = 6 . EXCAVATED JOINT

| | | | |
|---|---|---|---|
| NEW MATERIAL FLAG = | 2 | NORMAL STIFFNESS = | 1.00E+03 |
| RESIDUAL FRICTION = | 0. | SHEAR STIFFNESS = | 1.00E+02 |
| TENSILE STRENGTH = | 1.00E+10 | MAXIMUM CLOSURE = | 2.00E+02 |
| CPSTAR = | 0. | PEAK COHESION = | 1.00E+10 |
| INITIAL DILATION ANGLE = | 0. | RESIDUAL COHESION = | 1.00E+10 |
| CRITICAL NORMAL STRESS = | -1.00E+10 | | |

| NODAL POINT | TYPE | R-ORIGINAL | Z-ORIGINAL | R-LOAD OR DISPLACEMENT | Z-LOAD OR DISPLACEMENT |
|---|---|---|---|---|---|
| 1 | 2 | 0. | 0. | 0. | 0. |
| 2 | 2 | 13.000 | 0. | 0. | 0. |
| 3 | 3 | 25.000 | 0. | 0. | 0. |
| 4 | 2 | 33.400 | 0. | 0. | 0. |
| 5 | 2 | 33.400 | 0. | 0. | 0. |
| 377 | 0 | 12.000 | 70.000 | 0. | 0. |
| 378 | 0 | 25.000 | 70.000 | 0. | 0. |
| 379 | 0 | 34.750 | 70.000 | 0. | 0. |
| 380 | 0 | 43.000 | 70.000 | 0. | 0. |
| 381 | 0 | 50.000 | 70.000 | 0. | 0. |

| NODAL POINT | TYPE | R-CURRENT | Z-CURRENT | R-LOAD OR DISPLACEMENT | Z-LOAD OR DISPLACEMENT |
|---|---|---|---|---|---|
| 1 | 2 | 0.009 | 0. | 0. | 0. |
| 2 | 2 | 13.000 | 0. | 0. | 0. |
| 3 | 3 | 25.000 | 0. | 0. | 0. |
| 4 | 2 | 33.400 | 0. | 0. | 0. |
| 5 | 2 | 33.400 | 0. | 0. | 0. |
| 377 | 0 | 12.010 | 69.990 | 0. | 0. |
| 378 | 0 | 25 010 | 69.990 | 0. | 0. |
| 379 | 0 | 34.750 | 69.990 | 0. | 0. |
| 380 | 0 | 43.000 | 69.990 | 0. | 0. |
| 381 | 0 | 50.000 | 69.990 | 0. | 0. |

| ELEMENT | I | J | K | L | MATERIAL |
|---|---|---|---|---|---|
| 1 | 5 | 14 | 13 | 4 | 4 |
| 2 | 14 | 27 | 26 | 13 | 4 |
| 3 | 27 | 46 | 45 | 26 | 4 |
| 4 | 46 | 66 | 65 | 45 | 4 |
| 5 | 66 | 93 | 92 | 65 | 4 |
| 378 | 369 | 370 | 379 | 378 | 1 |
| 379 | 370 | 371 | 380 | 379 | 1 |
| 380 | 371 | 372 | 381 | 380 | 1 |
| 381 | 134 | 135 | 174 | 174 | 1 |
| 382 | 94 | 95 | 137 | 137 | 1 |

BANDWIDTH = 92

PRESSURE BOUNDARY CONDITIONS

| I | J | PRESS. I | PRESS. J |
|---|---|---|---|
| 381 | 380 | 9.69E+06 | 9.69E+06 |
| 380 | 379 | 9.69E+06 | 9.69E+06 |
| 379 | 378 | 9.69E+06 | 9.69E+06 |
| 378 | 377 | 9.69E+06 | 9.69E+06 |
| 377 | 376 | 9.69E+06 | 9.69E+06 |
| 80 | 56 | 1.30E+07 | 1.31E+07 |
| 56 | 36 | 1.31E+07 | 1.32E+07 |
| 3[illegible] | 21 | 1.32E+07 | 1.34E+07 |
| 2[illegible] | 10 | 1.34E+07 | 1.36E+07 |
| 10 | 1 | 1.36E+07 | 1.38E+07 |

RESTART CONDITIONS

| JOINT | N-STRESS | T-STRESS | KSMOD | KNMOD |
|---|---|---|---|---|
| 1 | -1.41E+07 | -9.17E+05 | 2.70E+09 | 1.00E+11 |
| 2 | -1.42E+07 | -1.78E+06 | 2.70E+09 | 1.00E+11 |
| 3 | -1.43E+07 | -2.24E+06 | 2.70E+09 | 1.00E+11 |
| 4 | -1.32E+07 | -2.67E+06 | 2.70E+09 | 1.00E+11 |
| 82 | -9.26E+06 | -2.59E+06 | 2.70E+09 | 1.00E+11 |
| 83 | -1.29E+07 | -2.90E+06 | 2.70E+09 | 1.00E+11 |
| 84 | -1.24E+07 | -2.95E+06 | 2.70E+09 | 1.00E+11 |
| 85 | -1.18E+07 | -2.77E+06 | 2.70E+09 | 1.00E+11 |

This is a Restart from Run 1. Solid and Joint Restart Stresses are Given

| ELEMENT | R-STRESS | Z-STRESS | RZ-STRESS | EMOD | ANUMOD |
|---|---|---|---|---|---|
| 86 | -1.40E+07 | -7.51E+06 | 2.12E+05 | 3.00E+10 | 2.50E-01 |
| 87 | -1.50E+07 | -1.03E+07 | 5.96E+05 | 3.00E+10 | 2.50E-01 |
| 88 | -1.46E+07 | -1.16E+07 | 6.65E+05 | 3.00E+10 | 2.50E-01 |
| 89 | -1.47E+07 | -1.08E+07 | 1.03E+05 | 3.00E+10 | 2.50E-01 |
| 90 | -1.45E+07 | -1.03E+07 | -1.30E+05 | 3.00E+10 | 2.50E-01 |
| 379 | -1.20E+07 | -9.77E+06 | -1.37E+04 | 3.00E+10 | 2.50E-01 |
| 380 | -1.17E+07 | -9.56E+06 | -1.99E+05 | 3.00E+10 | 2.50E-01 |
| 381 | -1.69E+07 | -1.09E+07 | 1.71E+06 | 3.00E+10 | 2.50E-01 |
| 382 | -1.58E+07 | -9.11E+06 | 5.01E+05 | 3.00E+10 | 2.50E-01 |

ITERATION NUMBER 1

SHEAR STIFFNESS OF THE DILATANT JOINTS

| JOINT NUMBER | KSMOD |
|---|---|
| 1 | 2.710E+09 |
| 2 | 2.710E+09 |
| 3 | 2.710E+09 |
| 4 | 2.713E+09 |
| 81 | 2.710E+09 |
| 82 | 2.727E+09 |
| 83 | 2.714E+09 |
| 84 | 2.715E+09 |
| 85 | 2.717E+09 |

In a dilatant case, iteration 1 is used only to set up the calculations.

It updates the shear stiffness of the dilatant joints, and the stiffness of the transverse restraint to each joint (KNEFF).

EFFECTIVE STRUCTURAL STIFFNESS PERPENDICULAR TO THE DILATANT JOINTS

| JOINT NUMBER | KNEFF |
|---|---|
| 1 | 1.039E+11 |
| 2 | 9.297E+10 |
| 3 | 1.081E+11 |
| 81 | 1.144E+11 |
| 82 | 1.050E+11 |
| 83 | 9.752E+10 |
| 84 | 1.149E+11 |
| 85 | 9.892E+10 |

ITERATION NUMBER 2

In this case, iteration 2 is the first one in which displacements and stresses are calculated.

| NODE | CURRENT R-DISPL | CURRENT Z-DISPL |
|---|---|---|
| 1 | 1.496E-04 | 0. |
| 2 | 1.018E-04 | 0. |
| 3 | 0. | 0. |
| 4 | -2.223E-05 | 0. |
| 378 | 5.101E-04 | -1.735E-05 |
| 379 | 7.658E-04 | -1.523E-04 |
| 380 | 9.134E-04 | -4.659E-04 |
| 381 | 8.563E-04 | -5.779E-04 |

| ELEMENT | R | Z | R-STRESS | Z-STRESS | RZ-STRESS | MAX-STRESS | MIN-STRESS | ANGLE |
|---|---|---|---|---|---|---|---|---|
| 86 | 6.50 | 4.10 | -1.39E+07 | -7.10E+06 | 1.57E+05 | -7.10E+06 | -1.40E+07 | 88.85 |
| 87 | [illegible]00 | 4.10 | -1.52E+07 | -1.04E+07 | 7.27E+05 | -1.03E+07 | -1.53E+07 | 81.71 |
| 8[illegible] | [illegible].17 | 4.10 | -1.49E+07 | -1.18E+07 | 7.59E+05 | -1.16E+07 | -1.50E+07 | 76.84 |
| 89 | 32.13 | 4.10 | -1.49E+07 | -1.09E+07 | 9.77E+04 | -1.08E+07 | -1.49E+07 | 88.79 |
| 90 | 39.70 | 4.10 | -1.47E+07 | -1.06E+07 | -2.31E+05 | -1.06E+07 | -1.47E+07 | -86.97 |

| TENFAC | SHFAC | NEXT EMOD |
|---|---|---|
| 1.00E+10 | 1.08E+01 | 3.00E+10 |
| 1.00E+10 | 1.28E+01 | 3.00E+10 |
| 1.00E+10 | 1.43E+01 | 3.00E+10 |
| 1.00E+10 | 1.36E+01 | 3.00E+10 |
| 1.00E+10 | 1.35E+01 | 3.00E+10 |

| ELEMENT | R | Z | NORMAL STRESS | TANGENT STRESS | NORMAL DISPL | TANGENT DISPL | NEXT KN |
|---|---|---|---|---|---|---|---|
| 1 | 31.35 | 4.10 | -1.46E+07 | -1.09E+06 | -2.14E-06 | -6.34E-05 | 1.00E+11 |
| 2 | 28.15 | 10.60 | -1.46E+07 | -2.03E+06 | 4.35E-07 | -9.16E-05 | 1.00E+11 |
| 3 | 25.50 | 16.00 | -1.49E+07 | -2.37E+06 | -3.57E-06 | -4.68E-05 | 1.00E+11 |
| 4 | 23.10 | 20.75 | -1.33E+07 | -2.50E+06 | 2.40E-06 | 6.22E-05 | 1.00E+11 |

| NEXT KS | SHFAC | DLNGL |
|---|---|---|
| 2.88E+09 | 1.42E+01 | 3.34 |
| 2.88E+09 | 7.61E+00 | 3.36 |
| 2.87E+09 | 6.68E+00 | 3.19 |
| 2.91E+09 | 5.70E+00 | 3.88 |

ITERATION NUMBER 4

Iteration 4 is the last one in Run 2. Hence, the cumulative displacements also are shown.

| NODE | CURRENT R-DISPL | CURRENT Z-DISPL |
|---|---|---|
| 1 | 1.519E-04 | 0. |
| 2 | 1.009E-04 | 0. |
| 3 | 0. | 0. |
| 4 | -1.752E-05 | 0. |

| NODE | CUMUL R-DISPL | CUMUL Z-DISPL |
|---|---|---|
| 1 | 9.316E-03 | 0. |
| 2 | 1.009E-04 | 0. |
| 3 | 0. | 0. |
| 4 | -1.752E-05 | 0. |

## 7. EXAMPLES OF APPLICATIONS

To illustrate the capabilities of the program, we present several examples of structures analyzed. Some of them were applications of earlier versions of the code, which did not have axisymmetric capability. These versions were:

JRC : plane analysis; no strain-softening; no dilation
JRCSTF : plane analysis; strain-softening; no dilation
JRCDLT : plane analysis, strain-softening; dilation effects

### 7.1 Jointed Mine Roof [JRC, 1967, (3)*.]

This was the first published application of any joint finite element. A mine roof was shown containing a single joint parallel to the horizontal roof. Depending upon the joint position, it was shown that the joint could be open (Fig. 11a), or closed (Fig. 11b) and that the immediate roof could be in compression (Fig. 11a) or in tension (Fig. 11b).

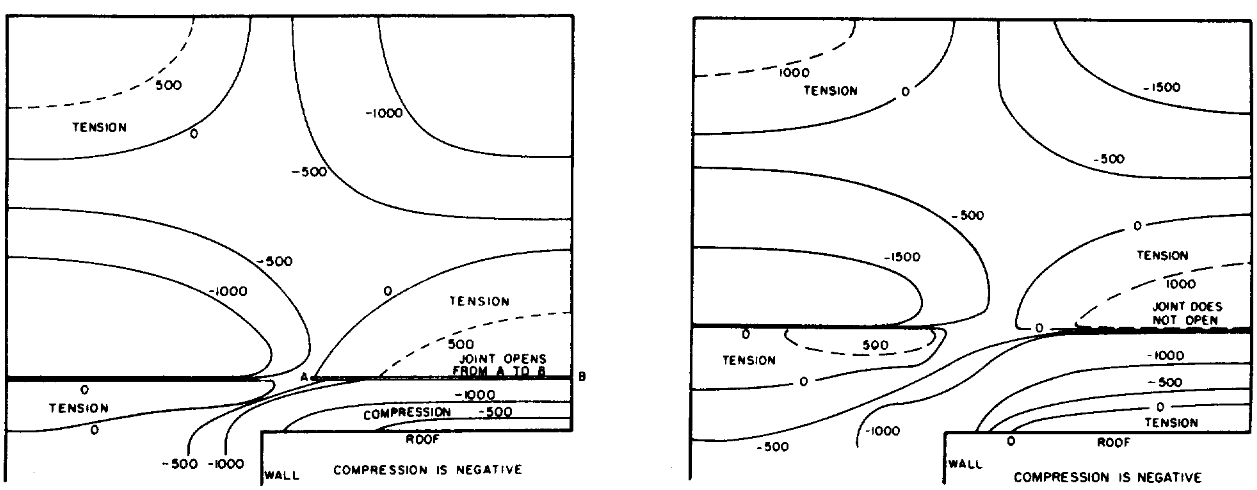


a) JOINT 5 ft ABOVE ROOF

b) JOINT 10 ft ABOVE ROOF

Figure 11: Horizontal Mine Roof With a Parallel Joint

---

*Reference number

7.2 Pile Driver Tunnels [JRCSTF, 1971, (4)]

Pile Driver was a nuclear weapons effects test in the Climax granite, at the Nevada Test Site (Fig. 12). Selected tunnel sections of the Pile Driver complex were analyzed under equivalent static loading. We obtained reasonably good agreement between observed and calculated closure and stability of the tunnels. Figure 13 shows Section BR12, where a discrete block is moving into the tunnel, along two joints.

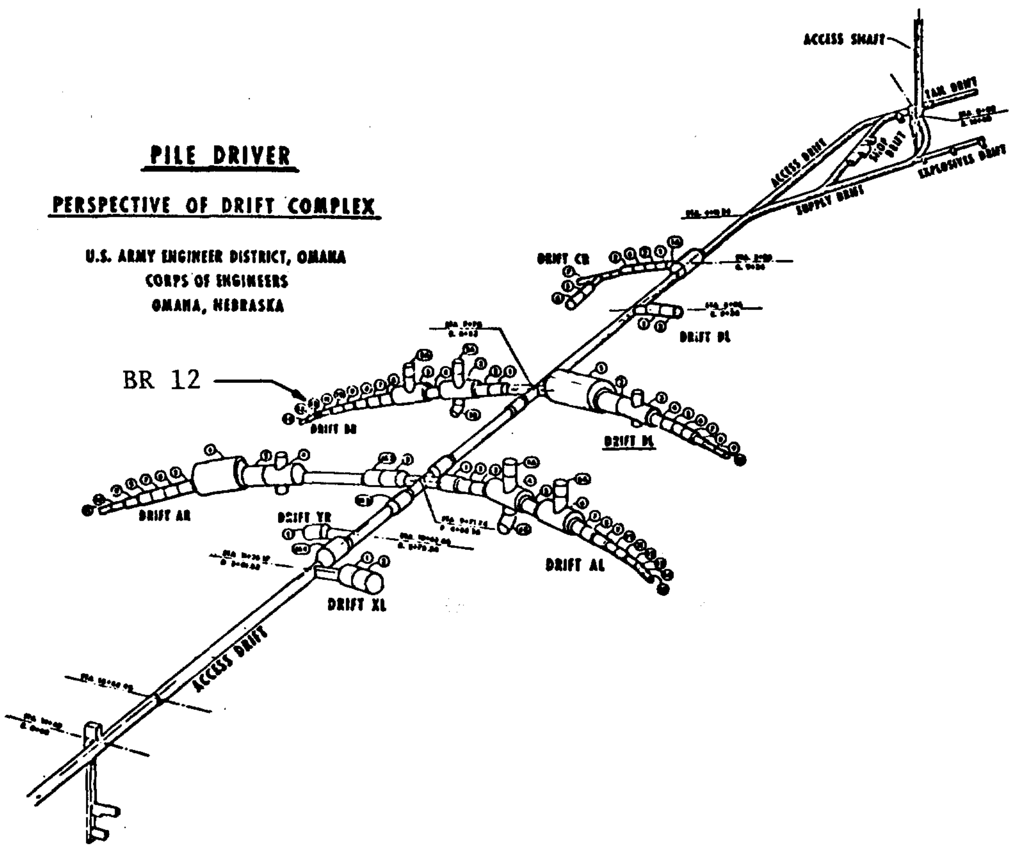


Figure 12: The Pile Driver Tunnel Complex, Nevada Test Site.

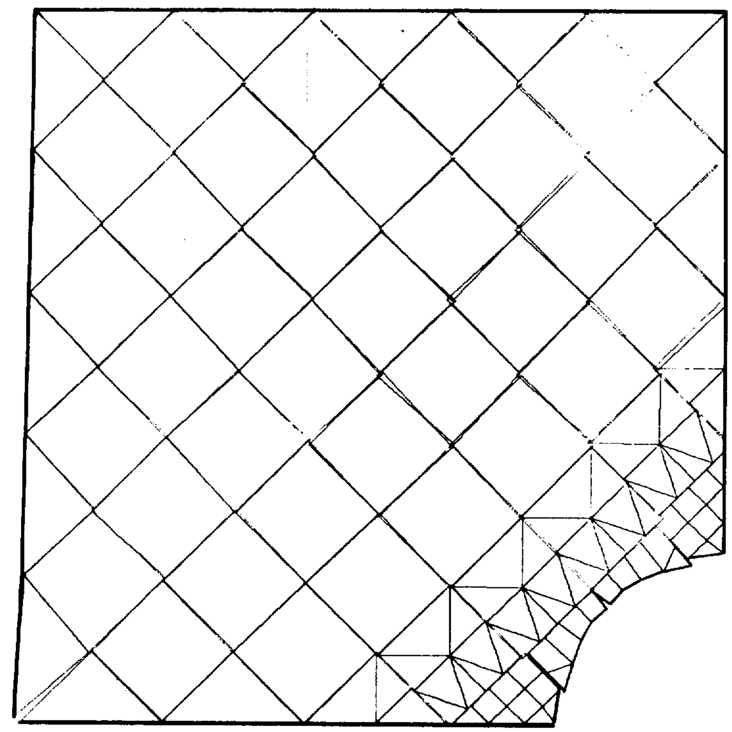

a) Displacements Magnified 5 Times

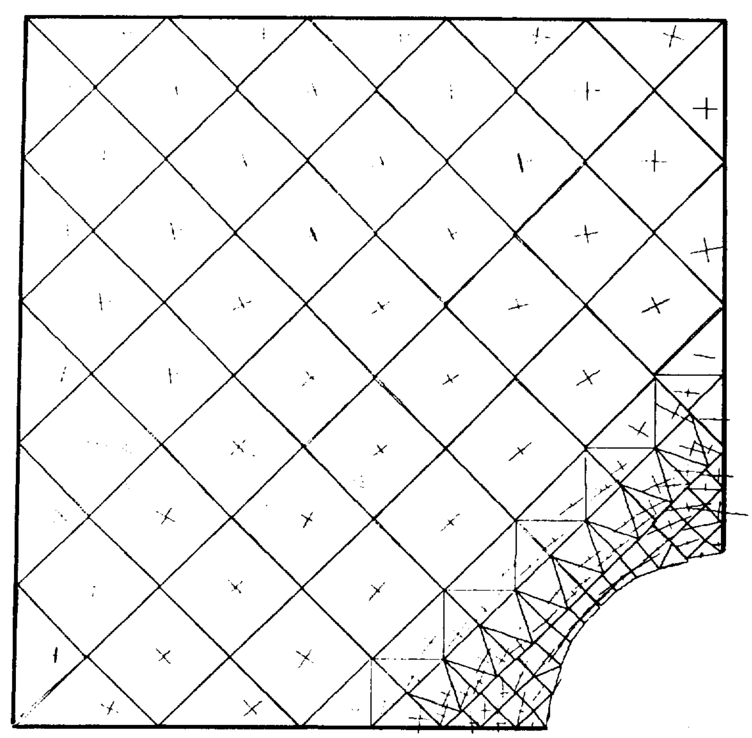

b) Stress Plot, and True Displacements

Figure 13: Models of the BR 12 Section, Pile Driver, NTS.

## 7.3 <u>Reinforced Tunnels in Bedded Rock</u> [JRCSTF, 1973, (5)]

The program was used to try and duplicate results obtained on scaled physical models of tunnels in bedded rock, reinforced by bolts and cables (Fig. 14). Although there was only fair agreement between the calculated values of tunnel closure, and the results from the physical models, the finite element models gave good repreentation of the rock failure around the tunnels and of the thrusting inward of the horizontal beds (Fig. 15).

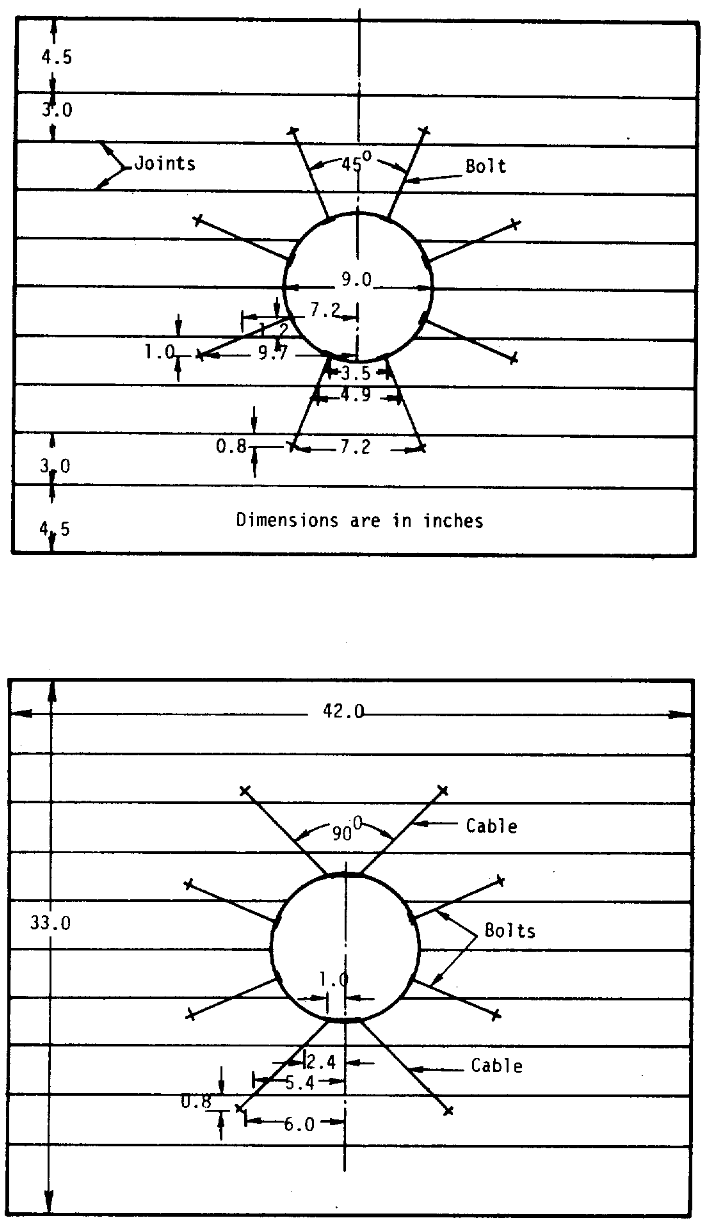


Figure 14: Sketch of Physical Models of a Tunnel in Bedded Rock, With Bolt and Cable Reinforcement.

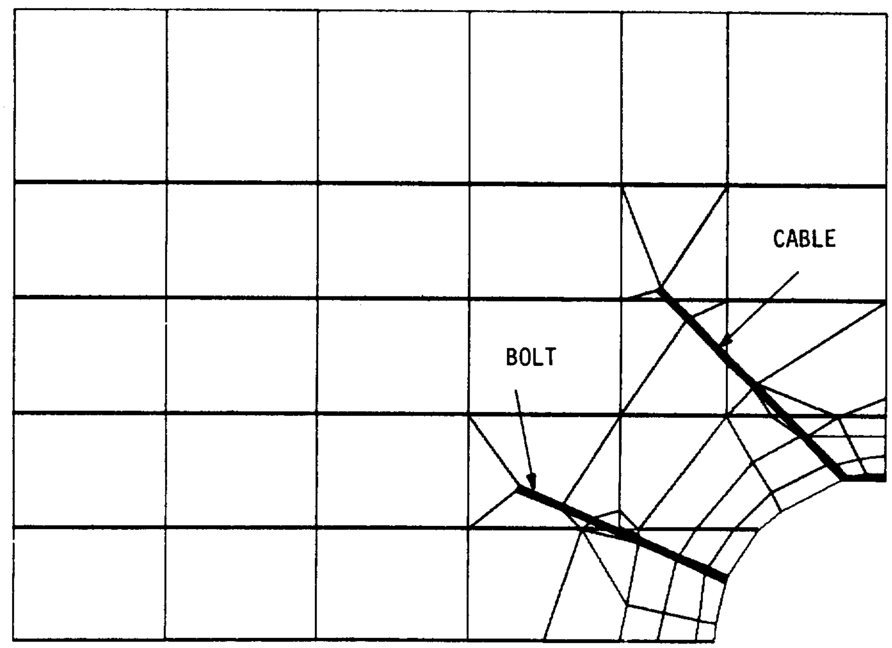


a) Finite Element Mesh, With Double Symmetry

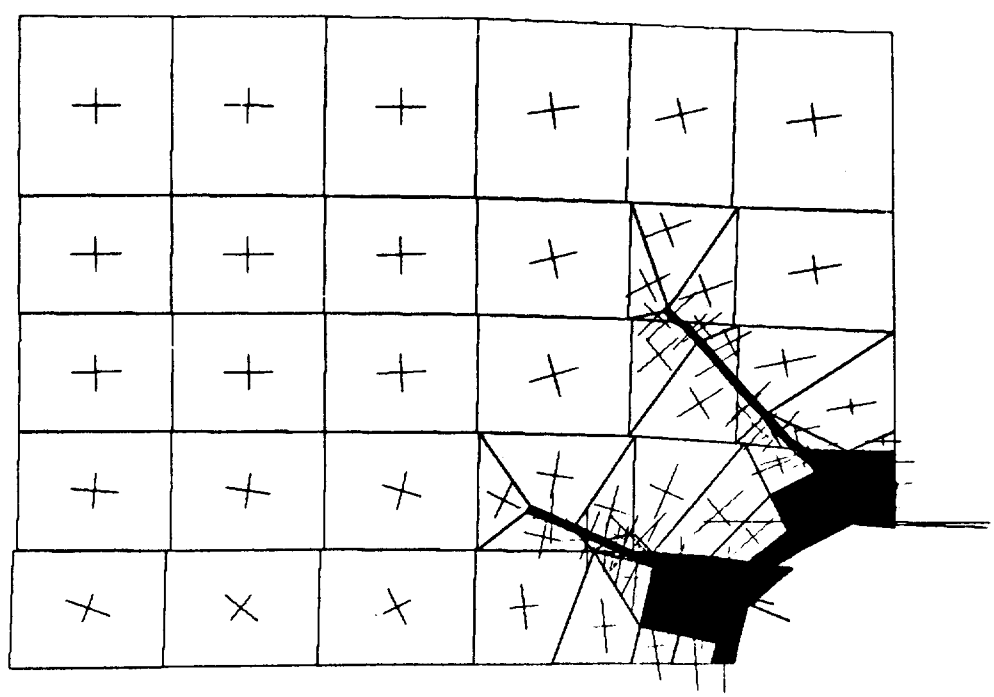

b) Principal Stress Plots. Dark Indicates Failure

Figure 15: Finite Element Models for the Structures on Figure 14.

## 7.4 Stiff Triaxial Test on Rock [JRCDLT, 1978, (6)]

An NX-core of Lyon's sandstone was tested in triaxial compression in the stiff system of the University of Colorado at Boulder. Strain control was achieved by means of steel posts loaded in parallel with the rock core (Fig. 16). By taking equivalent steel and rock area, a realistic plane model was built for analysis with JRCDLT. The comparison of experimental and calculated results (Fig. 17) showed the code's ability to model very pronounced strain-softening. Convergence was almost complete after five iterations. The axial load continued increasing in the first three iterations because of the horizontal slippage between the plates in the stacks, above and below the steel posts. Joint elements were used at the interfaces of these plates.

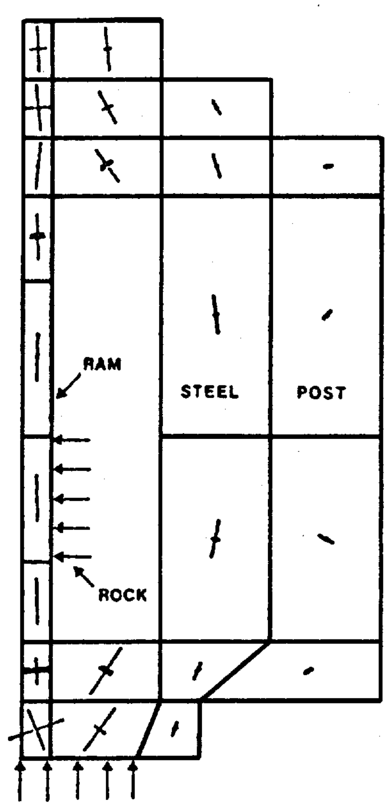


Figure 16: Stress Distribution in the Rock Sample and the Stiff Triaxial Steel System.

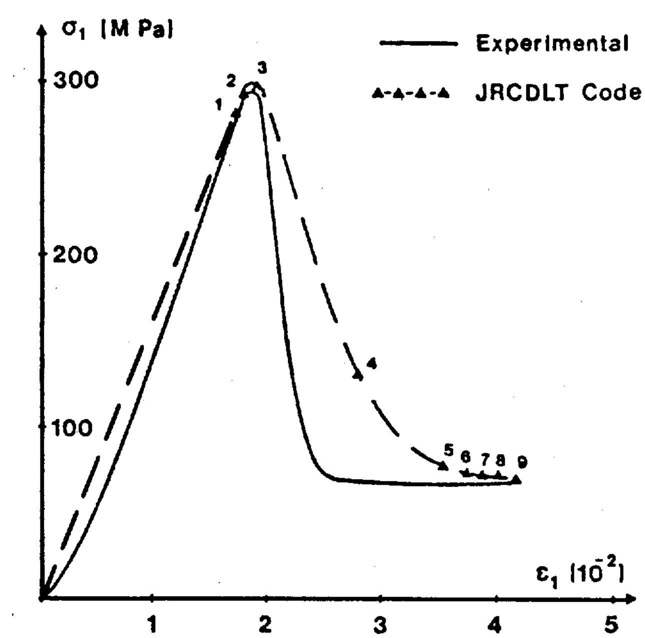


Figure 17: Comparison of the Observed and the Calculated Axial Response of the Rock Sample.

## 7.5 Atlanta's MARTA Peachtree Station [JRCSTF, 1979, (12)]

The main cavern of the Peachtree Center Subway Station in Atlanta, Georgia, was analyzed to evaluate its stability and the adequacy of the proposed rock bolt reinforcement. The model included several major joints and a number of bolts (Fig. 18). The calculations were instrumental in arriving at a final cavern design.

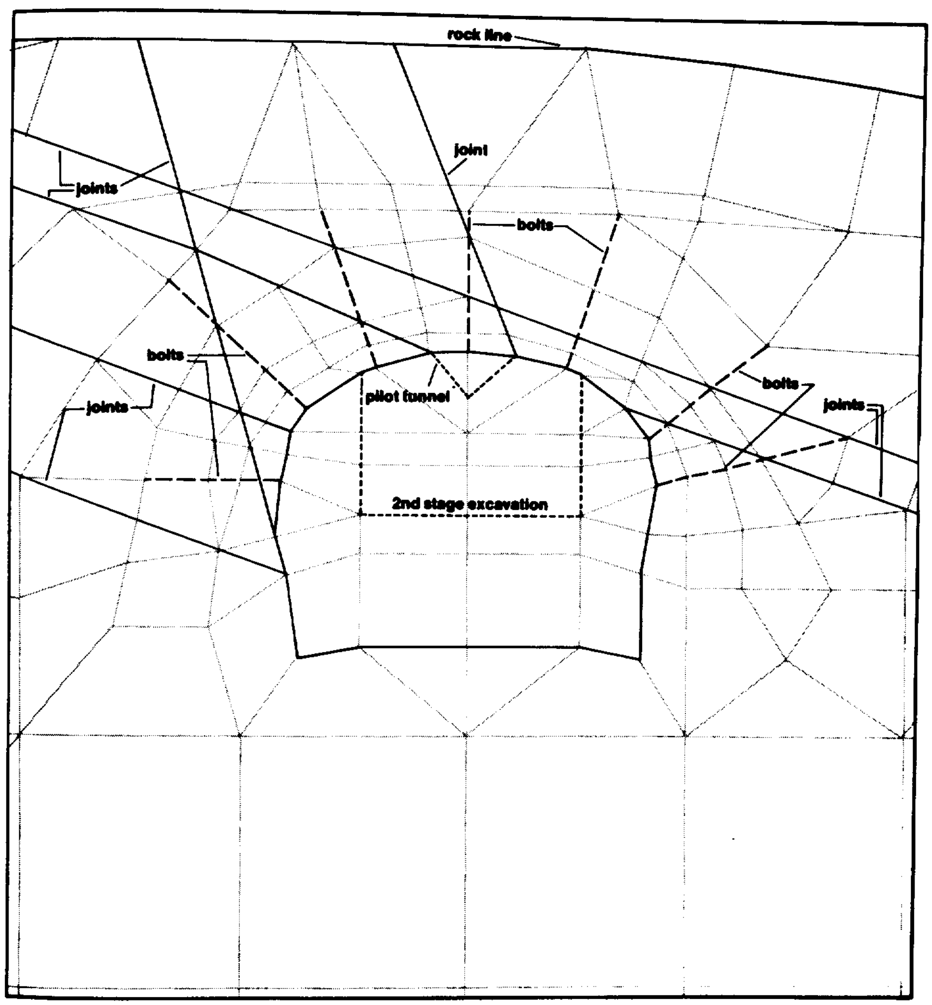


Figure 18: Model of the Cavern for Atlanta's Peachtree Station

7.6 Bureau of Mines Shear System [JRCDLT, 1979, (7)]

The U.S. Bureau of Mines in Denver developed a direct shear system in which the transverse stiffness, perpendicular to the shear plane, could be controlled (Fig. 19a). Results obtained with this machine clearly demonstrated the considerable influence of transverse restraint on joint shear strength.

A typical test was analyzed with a two-dimensional model of the machine (Fig. 19b). Calculations clearly showed the large increase in normal stress, $\sigma$, during shear displacement, u (Fig. 20). Under increasing normal stress, the dilation angle, $\delta$, steadily decreased (Fig. 21). The peak strength was increased several times over that which would be obtained if the initial normal stress had remained constant (Fig. 22).

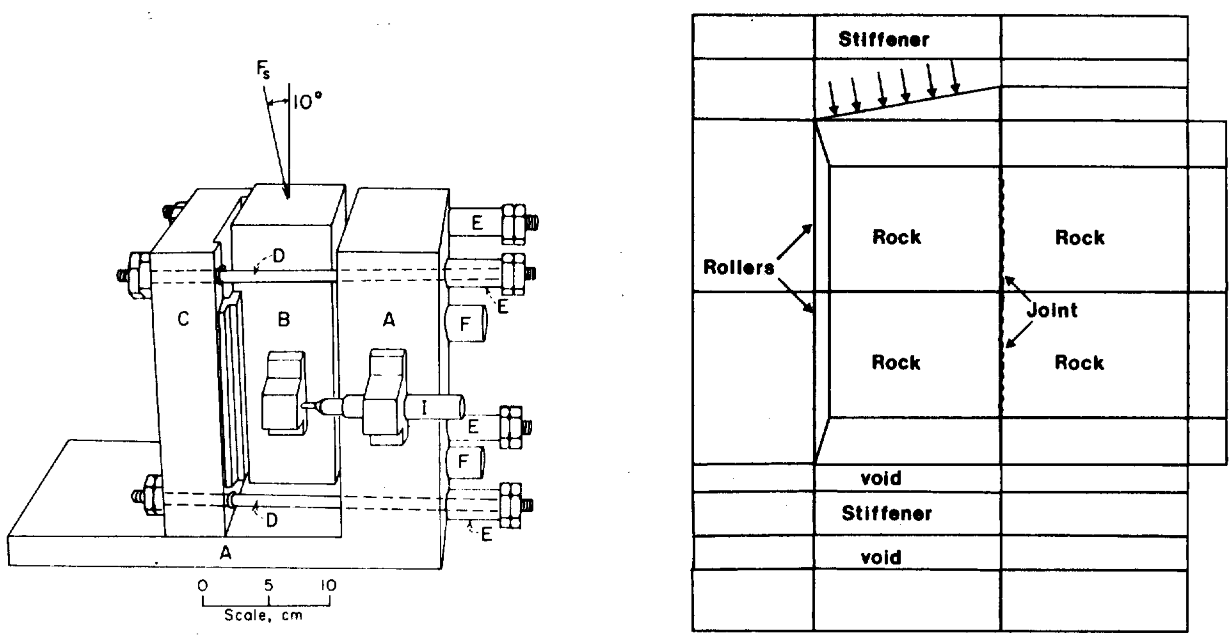


a) Sketch of Obert's Machine

b) 2-D Finite Element Approximation

Figure 19: Direct Shear Machine With Transverse Restraint.

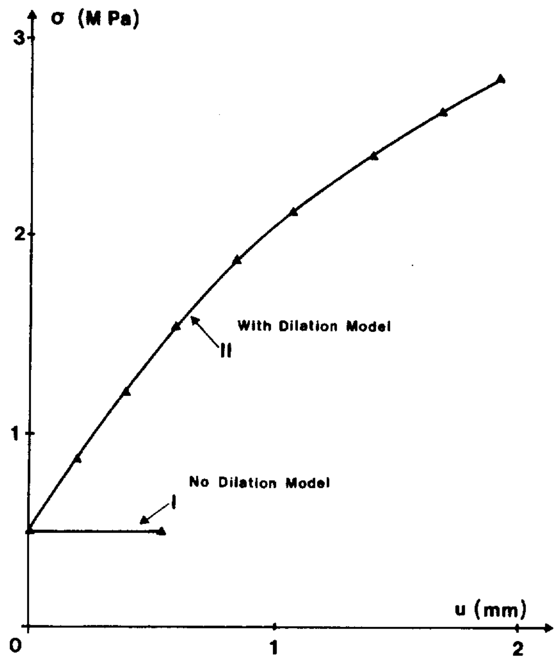


Figure 20: Increase in Normal Stress During Restrained Shear.

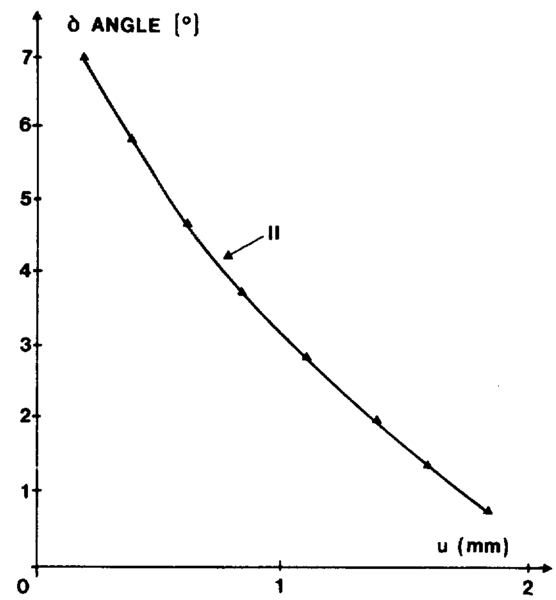


Figure 21: Decrease in Dilation Angle During Restrained Shear.

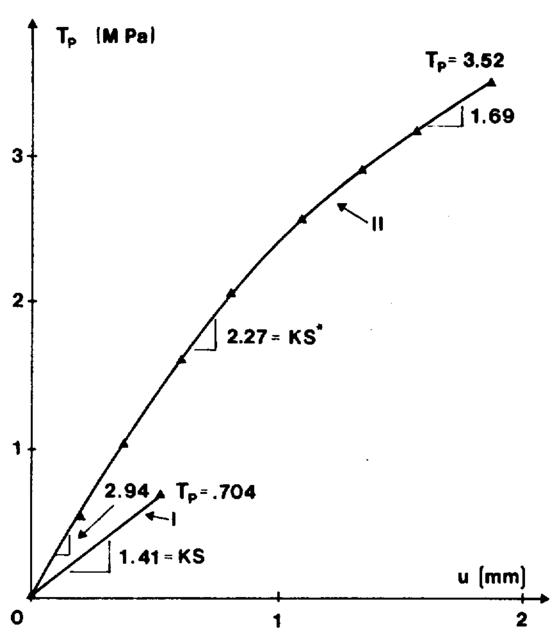


Figure 22: Large Increase in Shear Strength Created by Joint Dilatancy.

7.7 <u>Inguri Underground Cavern, USSR</u> [JRCDLT, 1979, (7)]

This model was proposed to the author by Dr. S. Yufin, visiting from the Moscow Institute of Civil Engineering. The cavern is shown in Fig. 23. It is 32 m wide. Comparison of results for rock movements and shear factors of safety of bolts are given in Figs. 24 to 26, under two different assumptions: friction = 45°, zero dilation, and friction = 35° plus 10° dilation. The effects of explicit modeling of the dilation were shown to be very pronounced. Figure 27 shows plots of the four-step sequence of excavation.

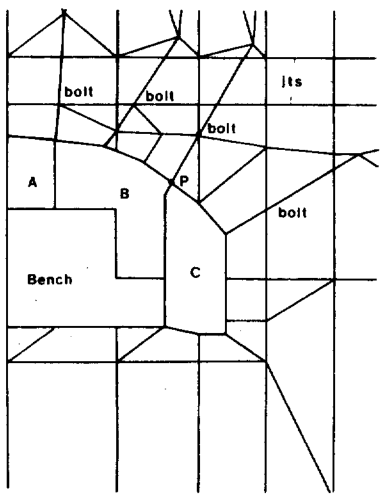


Figure 23: Model of Inguri Cavern.

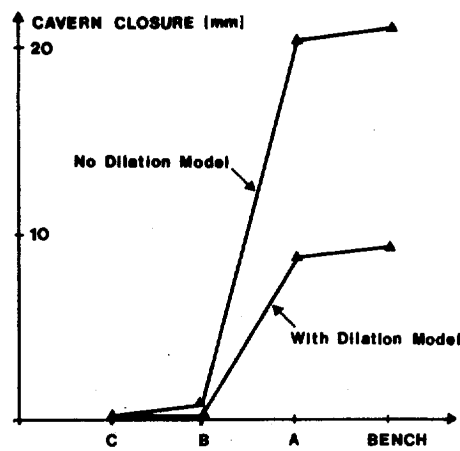


Figure 24: Vertical Cavern Closure During Excavation Sequence.

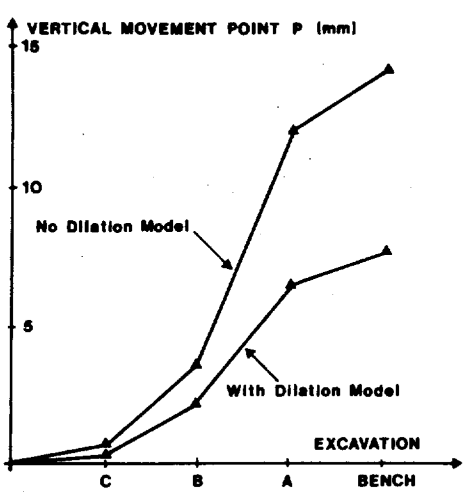


Figure 25: Vertical Displacement of a Selected Point.

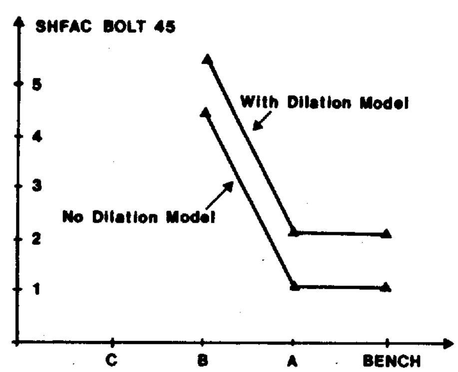


Figure 26: Shear Factor of Safety of Bolt Crossing a Joint.

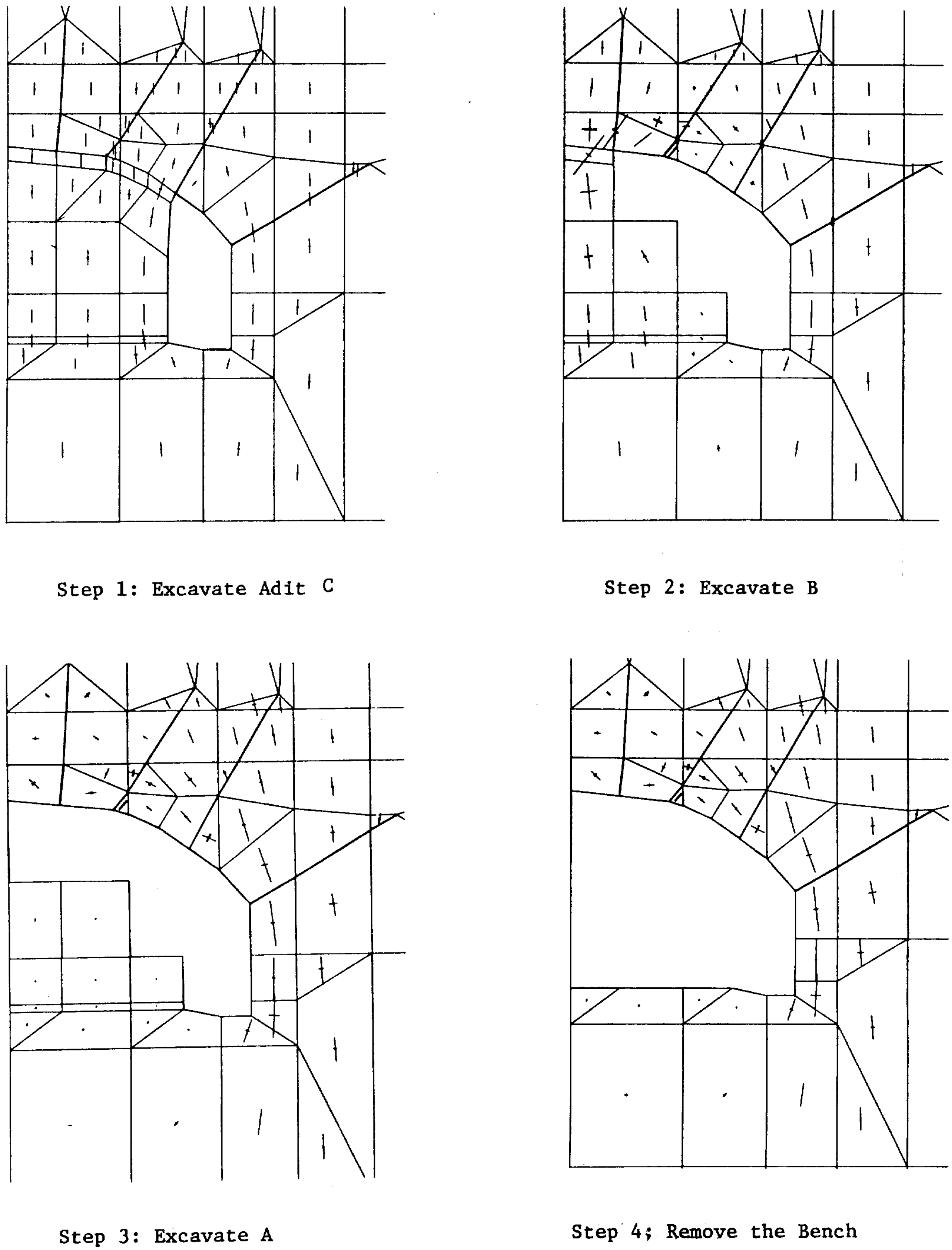


Figure 27: Principal Stresses During Sequential Excavation of the Cavern.

## 7.8 Shaft in Horizontally Bedded Rock [JPLAXD, 1979, (8)]

This example demonstrated the use of the axisymmetric joint element. Figure 28 shows a vertical shaft being sunk in horizontally bedded sandstones and siltstones. There are axisymmetric interfaces between the various rock beds. When the shaft is lined there is also an axisymmetric interface between the rock and the liner. Calculations were performed to show the influence of the horizontal to vertical stress ratio, $\sigma_H/\sigma_V$, and of the shear stiffness of bed interfaces, KS, on the shaft response. Figure 29 deals with the closure of an unlined shaft. As expected the stress ratio is very influential. Also the smoother bed interfaces allow more decoupling of the beds which translate into higher closure. Figure 30 shows the effect of the two parameters, $\sigma_H/\sigma_V$ and KS, on the circumferential stress on the liner. The effect of stress ratio is as expected. As for KS it is noteworthy that when beds are not decoupled (high KS) the newly excavated strata will drag the beds above them, when relaxing and will put a high stress on the liner.

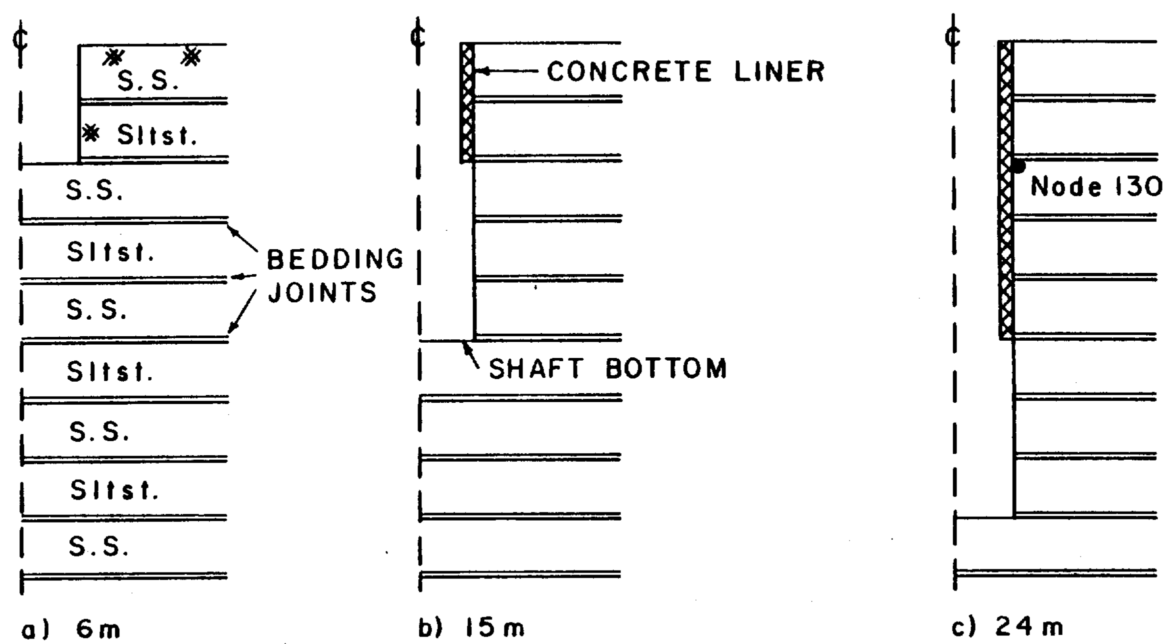


Figure 28: Excavation and Lining of a Vertical Shaft in Horizontal Strata

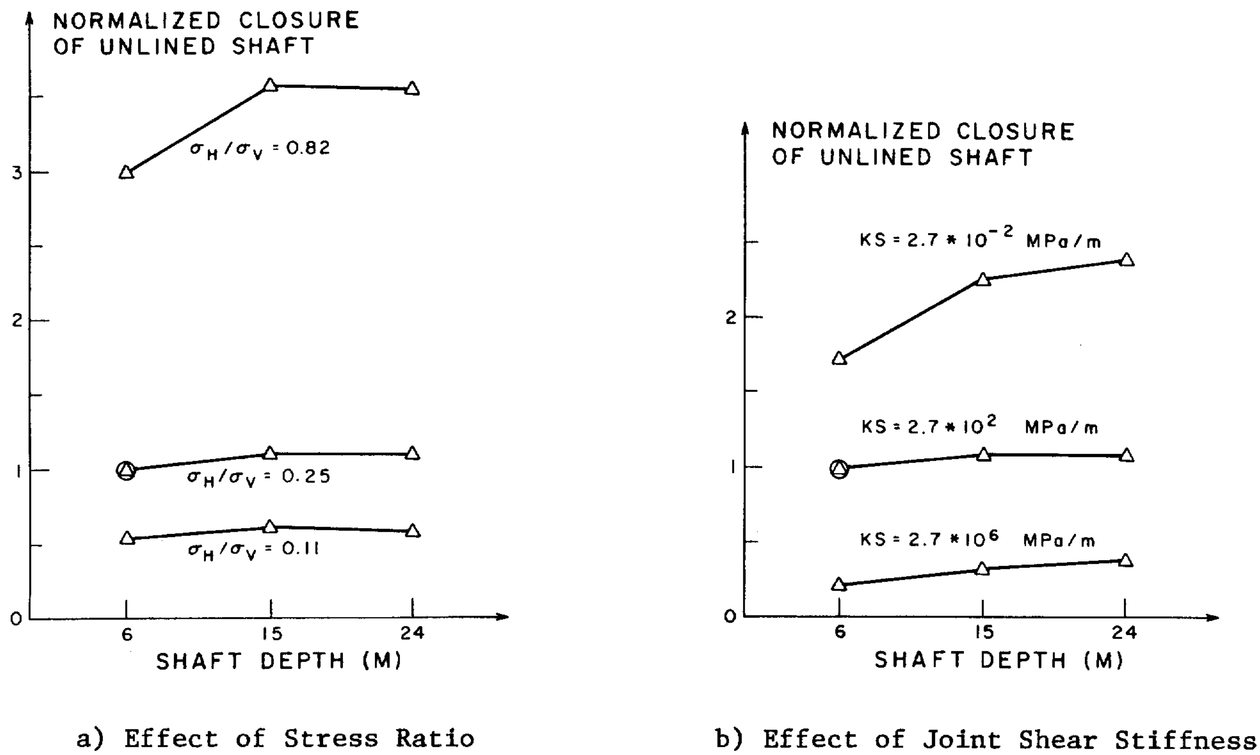


Figure 29: Closure of the Unlined Shaft.

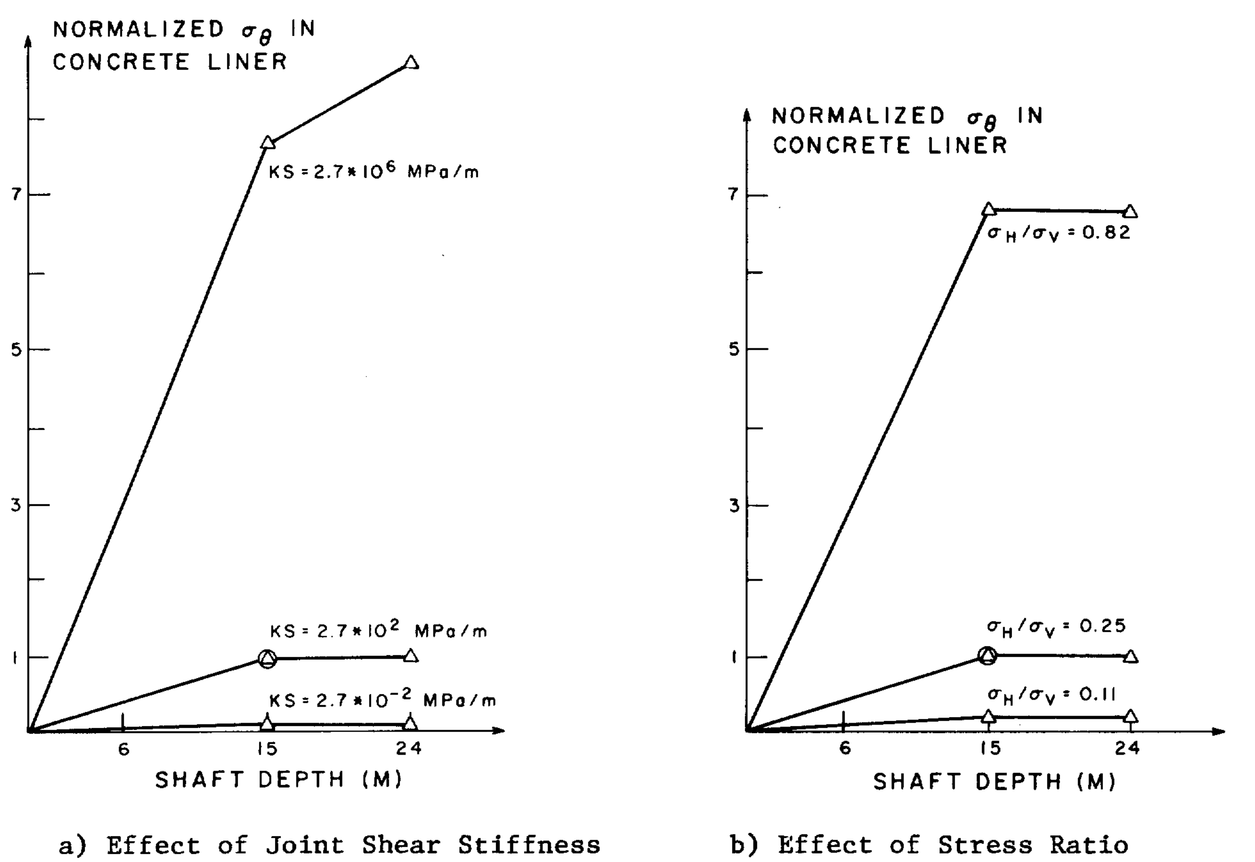


Figure 30: Tangential Stress in the Liner.

7.9 Embedded Circular Footing [JPLAXD, 1980, (9)]

This was another example of analysis with axisymmetric joints. The embedded footing of Fig. 31 had both vertical and horizontal interfaces with its foundation. Fig. 32 illustrates how the vertical stress under the footing varies, depending upon whether discrete interfaces are modeled as such or not. The fully-bonded models underestimated the vertical stress; hence they underestimated the vertical settlement. This is unconservative.

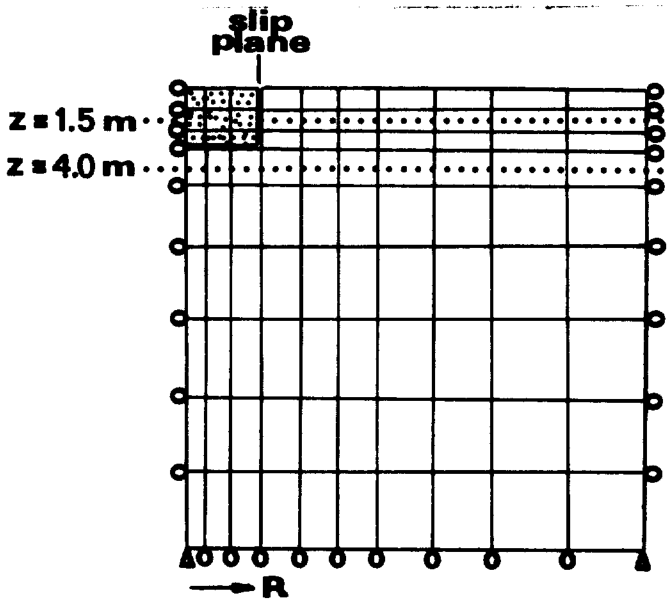


Figure 31: Model of Embedded Circular Footing

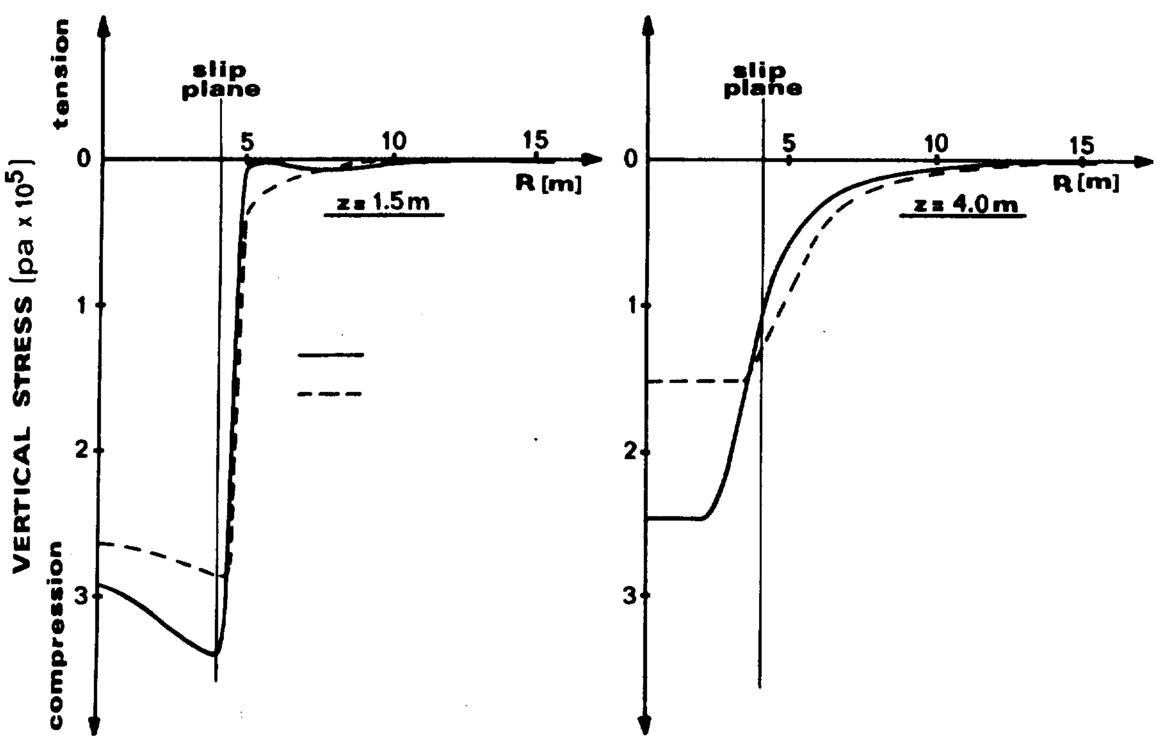


Figure 32: Vertical Stress Under the Footing.

7.10 Bolted Rock Slope [JPLAXD, 1981, (10)]

A rock slope was excavated in two steps (Fig. 33). Bolt reinforcement was installed after the top cut was made. The bolts could be tensioned or untensioned. Table 1 shows the calculated joint factor of safety against shear, depending upon the various assumptions.

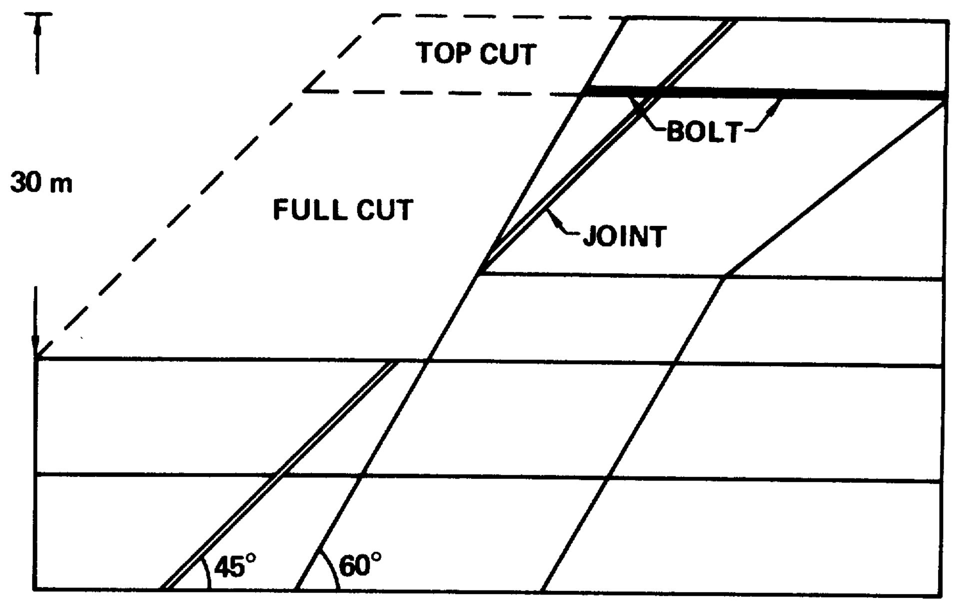


Figure 33: Model of a Bolted Rock Slope.

Table 1

SHEAR FACTOR OF SAFETY FOR THE JOINTED ROCK SLOPE

| CONDITION | DILATION ANGLE | SHEAR FACTOR OF SAFETY |
|---|---|---|
| No Bolt | $\delta_o = 0^o$ | 0.66 |
| No Bolt | $\delta_o = 10^o$ | 1.15 |
| Untensioned Bolt | $\delta_o = 0^o$ | 0.74 |
| Untensioned Bolt | $\delta_o = 10^o$ | 1.29 |
| Tensioned Bolt | $\delta_o = 0^o$ | 2.46 |
| Tensioned Bolt | $\delta_o = 10^o$ | 4.88 |

## 7.11 Climax Mine-By, Nevada Test Site [JPLAXD, 1981, (11)]

Three drifts were excavated in the context of the Spent Fuel Test, in the Climax granite, at the Nevada Test Site. JPLAXD was used successfully to explain stress changes in the rock pillars between the three caverns, which has not been duplicated by continuum models. Figure 34 shows the mesh used at Station 2+83; it had several discrete shears. Figure 35 shows principal stress plots during the sequential excavation.

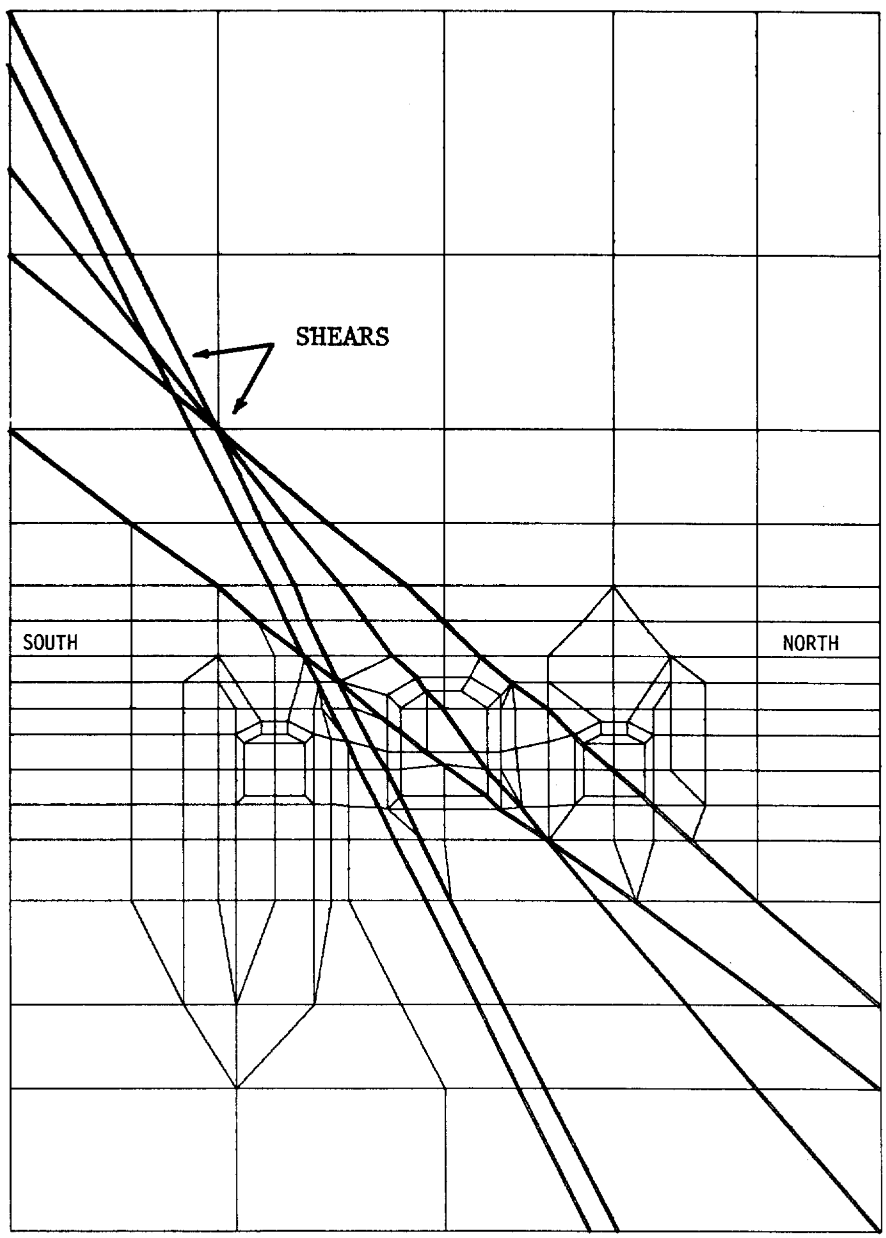


Figure 34: Model of Climax Spent Fuel Test, Station 2+83.

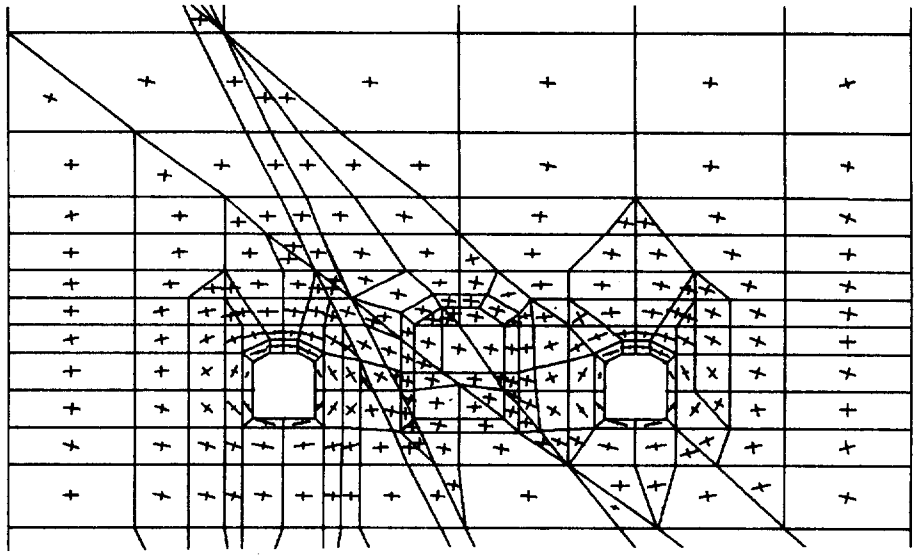

a) Excavation of the Side Drifts

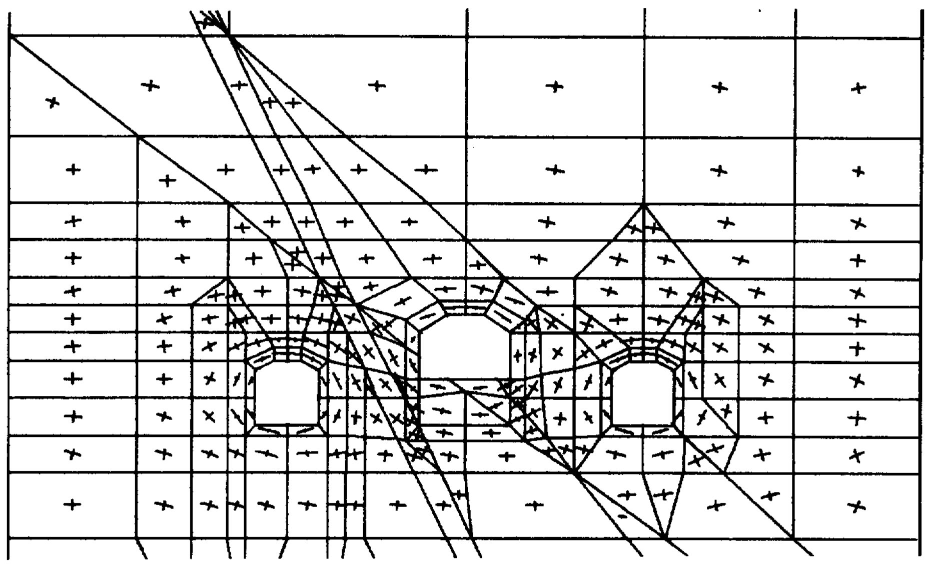

b) Excavating the Top Heading in the Center Drift

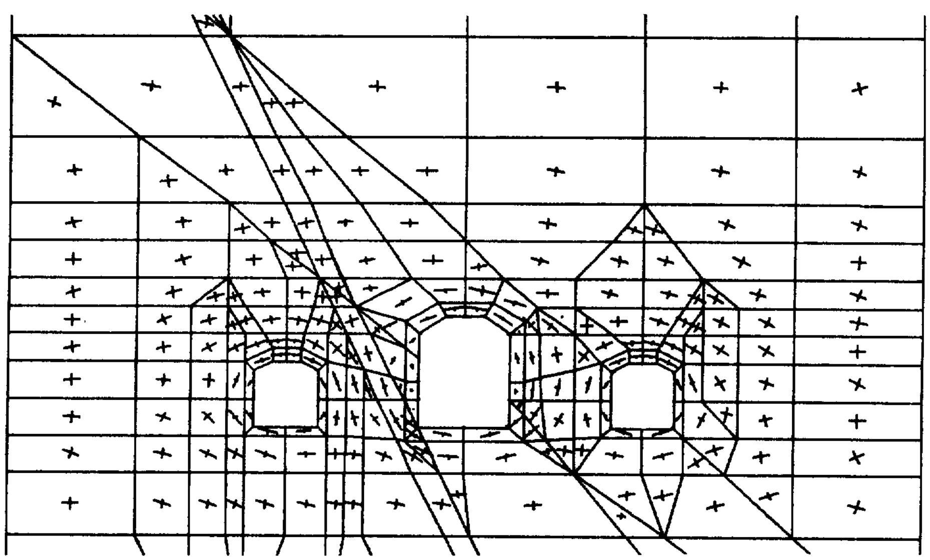

c) Bench of the Center Drift Removed

Figure 35: Principal Stresses During Excavation of the Climax Drifts.

## REFERENCES


1. Goodman, R. E. (1976) "Methods of Geological Engineering", West Publishing Co.,

2. Goodman, R. E., et al. (1968) "A Model for the Mechanics of Jointed Rock", J. Soil Mech. and Found. Div., ASCE, SM3, May, pp 637-659.

3. Heuze, F. E. and Goodman, R. E. (1967) "Mechanical Properties and In-Situ Behavior of the Chino Limestone, Crestmore Mine, Riverside, California", Proc. 9th U.S. Symp. on Rock Mechanics, Golden, Colorado, AIME Ed., pp 181-202.

4. Heuze, F. E. and Goodman, R. E. (1971) "Finite Element Studies of Piledriver Tunnels Including Considerations of Support Requirement", Report to U.S. Army Corps of Engineers, Omaha on Contract DACA 45-71-C-0031, v. 1, Aug., 129 p.

5. Heuze, F. E. and Goodman, R. E. (1973) "Numerical and Physical Modeling of Reinforcement Systems for Tunnels in Jointed Rock", Report to U.S. Army Corps of Engineers, Omaha on Contract DACA 45-72-C-0288, Aug., 106 p. (AD-766833).

6. Heuze, F. E. and Barbour, T. G. (1978) "Stability Analysis for Rock Structures", Proc. 19th U.S. Symp. on Rock Mechanics", Stateline, Nev., U. of Nevada, Reno, Ed., pp 452-460.

7. Heuze, F. E. (1979) "Dilatant Effects of Rock Joints", Proc. 4th Congress Int. Soc. for Rock Mechanics, Montreux, Switz., Sept., v. 1, pp 169-175.

8. Heuze, F. E. (1979) "Analysis of Circular Shafts in Sedimentary Rocks", SME/AIME Fall Meeting, Tucson, Arizona, Oct., Preprint 79-316.

9. Heuze, F. E. and Barbour, T. G. (1980) "New Models for Rock Joints and Interfaces", Lawrence Livermore National Laboratory, Report UCRL-85222.

10. Heuze, F. E. (1981) "Analysis of Bolt Reinforcement in Rock Slopes", Proc. 3rd Int. Conf. on Stability in Surface Mining, Vancouver, B. C. June. Available as Lawrence Livermore National Laboratory Report UCRL-85871.

11. Heuze, F. E. (1981) "Geomechanics of the Climax Mine-By, Nevada Test Site", Proc. 22nd U. S. Symposium on Rock Mechanics, Cambridge, Mass, July. Available as Lawrence Livermore National Laboratory Report UCRL-85768.

12. Kuesel, T. R. and King, E. H. (1979) "MARTA's Peachtree Center Station", Proc. 4th RETC Conference, Atlanta, GA., pp 1521-1544, AIME Ed.

13. Murrell, S. A. F. (1963) "A Criterion for Brittle Fracture of Rocks and Concrete Under Triaxial Stress, and the Effect of Pore Pressure on the Criterion", Proc. 5th U.S. Symposium on Rock Mechanics, Pergamon, pp. 563-577.

14. Obert, L. et al. (1976) "The Effect of Normal Stiffness on the Shear Resistance of Rock", Rock Mechanics, v. 8, pp 57-72.

15. Wilson, E. L. (1963) "Finite Element Analysis of Two-Dimensional Structures", D. Eng. Dissertation, Civil Engineering, University of California, Berkeley. Structural Res. Lab. Report 63-2.

## ACKNOWLEDGMENTS

T. G. Barbour participated in the axisymmetric development and J. C. Peterson coded the transversely isotropic model. T. Butkovich ran the Spent Fuel Test sample problems. Their contributions are gratefully acknowledged. We also thank L. Burrow for her fine typing of the manuscript.